GAS-SOLID FLUIDIZATION IN ANNULUS

A Dissertation
submitted in partial fulfilment
of the requirements for the award of the Degree
of
MASTER OF ENGINEERING
in
CHEMICAL ENGINEERING
(PLANT AND EQUIPMENT DESIGN)

By :- S. S. RAMA KRISHNAN
Guided By :- DR. N. GOPAL KRISHNA

DEPARTMENT OF CHEMICAL ENGINEERING
UNIVERSITY OF ROORKEE
ROORKEE (U.P.)
1974

CERTIFICATE

CERTIFIED that the thesis entitled " GAS-SOLID FLUIDIZATION IN ANNULUS" which is being submitted by Shri S.S. RAMA KRISHNAN in partial fulfilment of the requirements for the award of the DEGREE OF MASTER OF ENGINEERING IN CHEMICAL ENGINEERING (PLANT AND EQUIPMENT DESIGN) at the University of Roorkee, is a record of the candidate's own work carried out by him under the supervision and guidance of the undersigned. The matter embodied in this thesis has not been submitted for the award of any other degree or diploma.

This is further certified that he has worked for a period of 6½ months from January , 1974 to July 15, 1974 for preparing this thesis at this University.

ROORKEE
July 22, 1974.

N. Gopalkrishnan

(N.GOPAL KRISHNA)
PROFESSOR AND HEAD
DEPARTMENT OF CHEMICAL ENGINEERING
UNIVERSITY OF ROORKEE, ROORKEE.

SUMMARY

The thesis entitled " GAS-SOLID FLUIDIZATION IN ANNULUS" is presented in seven Chapters.

In Chapter-I , a brief introduction to fluidisation and scope of the present work are presented.

Chapter-II contains the literature review pertaining to minimum fluidising velocity, pressure drop and baffled fluidised beds.

Chapter -III presents the equipments fabricated for conducting experiments in annulus and straight tube. Experimental procedures for the determination of physical properties of materials and for obtaining data in annulus and straight tube, are discussed.

Chapter-IV deals with the experimental data obtained on variation of pressure drop with air mass velocity in straight tubes for three materials viz., spherical glass beads, crushed calcite and bauxite, in the sizes ranging from 440, 628 and 927 microns.

Experimental data on variation of pressure drop with air mass velocity in annulus is presented in Chapter-V for identical conditions as in straight tube. The weight of the bed per unit cross-sectional area of annulus was kept the same as in the corresponding straight tube.

The pressure drop experienced in annulus was higher than that in a straight tube. There was noticeable circulation of the solid particles upwards through the centre and down along the wall of the column.

At velocities beyond minimum fluidising velocity, the bubble size was observed to be small in an annulus than in the corresponding straight tube.

Chapter-VI embodies the experimental results and correlations to predict minimum fluidising velocity (G_{mf}) and pressure drop at the onset of fluidisation (ΔP_{mf}) in an annulus. The two correlations are as follows.

1. $$\left[\frac{G_{mfA}}{G_{mf\ Leva}}\right] = 0.12 \left[\frac{D_A}{D_p}\right]^{0.55} \left[\frac{A_1}{A_2}\right]^{-1.90}$$

2. $$\Delta P_{mf} = 0.78 \left[\frac{D_A}{D_p}\right]^{-0.02} \left[Re_{mf}\right]^{0.04} \left[\frac{W}{A}\right]$$

In the annulus with a smaller area of cross-section, G_{mf} was found to increase appreciably with increasing bed weights.

Large sized particles required a higher value of G_{mf} and finer particles resulted in higher ΔP.

As the annulus size was decreased, the wall effect factor, D_A / D_p , was found to exert pronounced effect on the quality of fluidisation and on the values of G_{mf} and ΔP_{mf}.

Chapter -VII deals with the conclusion based on the present study and scope for further work.

--

ACKNOWLEDGEMENTS

The author deems it a proud privilege to work under the erudite and infalliable guidance of Dr. N. GOPAL KRISHNA, M.Sc.Tech., M.Ch.E.(Brooklyn)., Ph.D. (I.I.T.,Kharagpur), M.I.I.Ch.E., Professor and Head, Department of Chemical Engineering, University of Roorkee, Roorkee and expresses grateful thanks for his critical reviews at each stage in the preparation of this dissertation.

Acknowledgement is gratefully given to the following persons who have contributed in the success of this work :

To,

Dr. P.S. Panesar, Associate Professor, for providing necessary workshop facilities.

Shri N.J.Rao, Reader in Chemical Engineering, for his ready and unstinted help in so many ways throughout the course of this work.

Shri Surendra Kumar, Lecturer, who helped a great deal in computer programming.

Dr. K. Subba Raju, Assistant Professor, Indian Institute of Technology, Madras, for his keen interest and encouragement.

And finally, members of the staff of the Department of Chemical Engineering for their helpful attitude.

C O N T E N T S

--

NOMENCLATURE

A	Cross-sectional area of fluidizing column, Cm^2
A_1	Cross-sectional area of annulus, Cm^2
A_2	Cross-sectional area of outer tube in annulus, cm^2
D_1	O.D. of inner tube in annulus, cm.
D_2	I.D. of outer tube in annulus, cm.
D_{equ}	$=(D_2-D_1)$, equivalent diameter of annulus, cm
D_A	$= (D_{equ}/2)$, cm.
D_p	Diameter of particle, microns.
Fr	$= (U^2_{mf}/ g. D_p)$, Froude number, dimensionless.
g	$= 980$ cm/sec^2, acceleration of gravity
g_c	$= 980$ gm. cm/(gm-wt) sec^2, conversion factor.
G_f	Fluid mass velocity based on empty column, gm/cm^2.hr
G_{mf}	Fluid mass velocity at minimum fluidization gm/cm^2.hr
G_{mfA}	Minimum fluidising mass velocity in annulus, gm/cm^2.hr.
G_{mfLeva}	Minimum fluidising mass velocity given by Leva's Equation, Eq. 2.
k	Proportionality constant
L	Height of the solids bed, cm.
L_{mf}	Bed height at minimum fluidising condition, cm.
ΔP	Pressure drop across solids bed, gm/cm^2
ΔP_{mf}	Pressure drop at onset of fluidisation, gm/cm^2
ΔP_r	Pressure drop across the grid plate, gm/cm^2
Re_{mf}	$=(D_{equ} \cdot G_{mf}/ \mu)$, Reynold's number based on empty annular cross-section, dimensionless.

Re_p	$=(D_p \cdot G_f \cdot / \mu)$, particle Reynold's number, dimensionless.
S_r	per cent grid open area.
U_{mf}	Superficial fluid velocity at minimum fluidizing condition, cm/sec.
W	Weight of solids, gm.

Greek Symbols

ϵ_{mf}	Void fraction, in a bed at minimum fluidizing condition, dimensionless.
μ	Viscosity of gas, gm/cm.sec.
ρ_f, ρ_s	Density of fluid and solid respectively, gm/cm^3
$\Delta\pi$	$= \Delta P_{mf} / (W/A)$, dimensionless pressure drop
ϕ_s	= Sphericity of a particle, dimensionless.

--

INTRODUCTION

The principle of operation of gas-solids fluidised beds is now well known because of their wide use in the petroleum, heavy chemical and metallurgical industries. Fluidized beds have many attractive features, the solids are mobile and well mixed, heat transfer is good and temperature gradiants largely absent. However, the good mixing has its own disadvantages in that gas-solids counter-current flow is not possible in a single stage bed. Although fluidized beds were used as long ago as 1921 in the German Winkler gas generator it was not until the fluidized catalytic Cracker was developed in the U.S.A. in 1941 that they became widely used. Since then more and more use has been made of fluidised beds not only in catalytic processes but also in the heavy chemical and metallurgical fields, e.g. the Fluo-solids pyrites roaster, lime calciner and drier.

Despite the extensive use of such beds very many of the factors controlling their performance are not properly understood, for example why bubbles are formed, what is the gas flow pattern in the bubbles and why the heat transfer between the gas and the wall is so good. A better understanding of the important factors involved

ance of existing beds can be
lt.

l more of an art than a science.
lied to a bed of solid particles
at bed from a settled state where
rous solid, to a state where it
erties of flow and surface levelling
ships. It implies, too, that
ly mobile.

fluidization, where the whole of
as a homogeneous fluid is probably
ice the term is loosely applied to
ned to a large degree in a state
rent of fluid. Attempts to define
zation have been made[1,2], but the
d indeed it does not appear that
able to all cases can be made.

re presented by literature on this
on by gases follows a distinctly
ization by liquids. Prior to
d state, however, the functioning
ncreasing flow of gas is passed
solids resting on a support plate
eventually reached when the bed

can no longer remain stable as a static entity. At this particular gas velocity the individual particles loosen themselves from the permanent contact with each other, and become freely supported on the rising current of gas. As the gas velocity is further increased, the bed takes on a more and more "liquid" or "fluid" appearance. Each particle is no longer constrained to a definite position as in the fixed bed state, but is free to move through out the whole bed. The entire mass looks like a liquid in continual agitation, possessing a mobile but nevertheless definite interface between itself and the gas space above. Also, as the gas velocity is further increased, the particle circulation within the bed becomes more and more rapid, analogous to that of a well-stirred liquid.

At higher gas velocities the gas ceases to pass uniformly through the homogeneous gas-solid mixture. Excess gas now starts to flow through the system as pockets or bubbles relatively free of solid. In this state the system is very similar in appearance to that of a boiling liquid, a further similarity being the ejection of particles into the free space above the bed as the bubbles break the interface. When the gas velocity is made to exceed the particle terminal velocity, these ejec ted particles can never regain the main bed, and so the bed will gradually be completely e-ntrained in the flowing gas stream, as in pneumatic conveying.

The whole of the region between the fixed bed condition and pneumatic conveying is known as the fluidised state. The condition at low velocities, where the whole bed is entirely homogeneous, is sometimes called the state of incipient fluidization, whereas at higher gas velocities where bubbles of gas constituting a second phase appear, the condition is known as the boiling bed state. It is this latter type of fluidised bed which is largely employed in contemporary industrial applications of the technique.

A liquid can equally well be used as the fludizing medium, although at present this is of less commercial importance than the gas system. In liquid-solid systems an increase in flow rate above minimum fluidization usually results in a smooth, progressive expansion of the bed. Gross flow instabilities are damped and remain small, and large-scale bubbling or heterogeneity is not observed under normal conditions. This is 'homogeneous' or 'particulate' fluidization.

When, however, the activating fluid is a gas, only a limited degree of smooth expansion is reported, occurring just before incipient fluidisation. Thereafter, particles are thrown by up bubbles bursting at the bed surface and the action gets more and more violent as the flow rate is stepped up. Until the bed is transformed into swirling clusters of particles filling the fluidization vessel and ultimately being transported in the gas stream. This is "aggregative" or "bubbling" fluidization.

Wilhelm and Kwank[3] have suggested using the Froude group ($U_{mf}^2/ g. d_p$) as a criterion for the type of fluidization obtained, in general aggregative fluidization is obtained at values above unity and particulate fluidization at values below unity.

It is generally accepted that liquid-solid systems result in 'particulate fluidization' and gas-solid system in 'aggregative fluidization'. But in extreme cases it was found to be the otherway. For example, lead shot fluidized in water and hollow paper cubes fluidized in air resulted in aggregative and particulate fluidization respectively.

From a consideration of the stability equations for the bed-fluid interface, Romero and Johanson suggested that the criterion between the two modes of fluidization may be given by

$$(Fr_{mf})(Re_{p,mf}) \left(\frac{\rho_s-\rho_g}{\rho_g}\right) \left(\frac{L_{mf}}{d_t}\right) < 100 \text{ , particulate}$$

$$\text{-do-} \qquad > 100 \text{ , aggregative}$$

QUALITY OF FLUIDIZATION

Although the properties of solid and fluid alone will determine whether smooth or bubbling fluidization occurs, many factors influence the rate of solid mixing, the size of bubbles, and the extent of heterogeneity in the bed. These factors include bed geometry, gas flow rate, type of gas distributor, and vessel internals such as screens and baffles.

'Slugging' is a phenomenon strongly affected by the choice and design of the equipment. Gas bubbles coalesce and grow as they rise, and in a deep enough bed they may eventually become large enough to spread across the vessel. Thereafter the portion of the bed above the bubble is pushed upward, as by a piston. Particles rain down from the slug and it finally disintegrates. Slugging is usually undesirable since it lowers the performance potential of the bed for both physical and chemical operations. Slugging is especially serious in long, narrow fluidized beds. In such beds, beyond the point of the onset of fluidzation, the pressure drop will increase above the value calculated from the weight of the bed. The pressure excess over the theoretical value is due to friction between solids slugs and the wall of the vessel. Since one would expect the heavier solids to slug more readily, it may well be that such factors as particle shape and size distribution may also be involved.

position is defined as a function of time and the properties at any point of the bed are same. The only major drawback is that the batch systems are not suitable for large scale operations.

In single stage batch fluidized systems solids are handled as batches and gas is continuously passed through the bed. The time of operation is usually governed by the system requirements. The contact of the gas with solids is once through and the quality of solid product is uniform. The efficiency of operation specially with gas phase will be low. Depending on the gas velocity the system will be either in fixed bed state or at incipient fluidized state or fluidised state or at elutriation. Thus in single batch fluidised systems, the paramèters which govern the behaviour are :

(i) Solid and fluid characteristics.

(ii) Minimum fluidizing velocity and

(iii) Bed pressure drop.

The solid and fluid characteristics which effect the behaviour of the fluidised bed are solid particle size, shape, density and fluid density, and viscosity. These factors are normally utilised in the prediction of minimum fluidising velocity.

IMPORTANCE OF THE PRESENT STUDY

Where large quantities of heat must be transferred, for example, in exothermic or endothermic chemical reactions on catalytic surfaces, the fluid-solid process may be found advantageous. These types of reactions may also require rigid constant temperature control, which may be difficult to achieve with a stationary bed of catalyst. In addition, some reactions form hot spots in the bed and destroy the catalyst by sintering, decomposition, volatilisation of promoters, etc. Or, if channeling occurs, as is readily posible in fixed-beds, only part of the catalyst may be in active use, the catalyst contact time may be decreased and temperature control may prove to be difficult and inaccurate. The fluid process alleviates many of the temperature control and heat-transfer difficulties encountered in stationary beds.

Addition or removal of heat is done by passing either steam or cooling water. Units with internal heat-transfer elements are extensively used in industry. The external heat-transfer surfaces have severe limitations as far as ratio of heat-transfer surface to reactor volume is concerned, whereas internally heated or cooled reactors may be equipped with virtually any amount of heat-transfer surface. A simple vertical cylindrical tube or rod may be employed, as the internal heat-transfer element in view of its following salient features :

(a) simplicity of design

(b) ease of installation and removal

(c) no interference with emptying the bed

(d) no defluidized regions (dead spots) occur

(e) additional area is available for heat-transfer purposes

(f) rods of small diameter occupy only a small fraction of the volume of the bed.

Coaxial introduction of such a vertical tube in a cylindrical fluidising column alters the geometry of the column to result in an annulus. Formation of such an annulus affects the flow pattern. The two extra walls provided by the inner tube cause the change in velocity distribution of fluid. In a cylindrical tube the fluid velocity is about equal to zero at the two walls and is maximum at the center of the column. But on the other hand, due to presence of four walls, the fluid velocity is about equal to zero at four points in an annulus. Also the velocity of fluid will be maximum at the centres symmetrical to each other in the annulus.

Wall Effect

Based on observations made during fluidization studies, there have been certain reports on the influence of container wall on the fluidization phenomenon. Lewis et al[4] obtained pressure drops at the minimum fluidization velocity higher than the theoretical ones. Such deviations of experimental results from the theoretical ones were considered to be an indication of a frictional drag on the walls of the unit, and were found to be independent of the L/D ratio.

During a discussion on the physical basis of fluidisation, Hancock[5] observed that the velocity of flow is not uniform over the entire cross-section of the containing column, being faster at the centre and tending to zero at the wall surface. When the fluidisation phenomenon was observed, the particles close to the walls were seen to be falling continuously against a rising current, thereby promoting mixing and preventing any particle attaining a steady position. Such effects were referred by Hancock as wall effects on fluidised conditions.

Morse[6] found fluid beds of large or heavy particles to be inherently unstable with a strongtendency to segregate and to form a non-uniform bed containing rising currents of solids concentrates. Some of these currents were observed to be localised; others extended over the entire bed. The particles being elevated in these currents absorbed kinetic energy from the gas stream. This kinetic energy was eventually lost by collisions among particles and against the walls.

Schwartz and Smith[7] reported that velocity profile for gases flowing through a packed bed is not flat, but has a maximum value approximately one pellet diameter from the pipe wall. The maximum or peak velocity ranges upto 100%, higher than the center velocity as the ratio of tube diameter to particle diameter decreases. The divergence of the profile from the assumption of a uniform velocity is less than 20% for ratios of D_t/D_p of more than 30. Application of the theory based on the concept of momentum transfer and variation of void fraction with radial position, suggests that it is satisfactory to assume that void fraction is constant at its minimum value upto a distance of two pellet diameters from the wall. At larger radii void fraction increases rapidly.

At a differential distance from the wall the void fraction will approach unity, since the particles can make only a line or point contact with the column surface. Near the center of the column the bed should not be affected by the wall; hence in this central core void fraction will have a constant minimum value. How close to the wall it will remain constant is a function of the size of packing. If only void space is considered, the velocity profile would have a flat central section, with the velocity increasing on either side as the pipe wall is approached. Actually, the wall will exert a frictional force on the gas, so that the velocity again decreases and approaches a zero value right at the wall surface. The development of a theory for the velocity distribution is particularly difficult because of the complexities introduced by the packing.

If the concept of fluid flow in packed beds developed by Schwartz and Smith[7] is extended to an annular bed, it may be expected that maximum velocity may occur at a short distance from the wall and then decrease from that point in both directions, gradually toward the center, and sharply toward the wall. However, since the curvatures of the outer and inner tube are quite different from each other, the orientation and the void fraction of solids will be different from that in a cylindrical tube which in turn will affect the velocity distribution of fluid in the bed. Hence a knowledge of the velocity distribution in an annular fluidised bed is important in analysing the operation of catalytic reactors etc., for which a detailed study should be made.

Extra surface provided by the introduction of a vertical tube, increases the skin friction considerably which in turn increases the pressure drop across the bed. The particle movement is restricted appreciably and wall effect may be more. Hence inter-particle friction is greater which would require a higher velocity to unlock the particles at the onset of fluidisation condition.

The inner vertical surface may help in suppressing the rate of bubble growth by breaking the bubbles at the

CHAPTER II

LITERATURE REVIEW

Minimum fluidising velocity (Gmf) may be defined[8] as the mass flow rate of fluid sufficient to start the expansion of the bed whose particles are arranged in the most loosely packed but still stable bed configuration. This mass flow rate usually coincides with the flow rate at the intersection of the fixed bed pressure gradient line and the isobaric fluid bed pressure drop line if channeling does not occur.

Gmf not only sets a lower limit on gas rate to the fluidised bed, but also is useful for prediction of bed expansion, for calculating heat transfer rates, in the analysis of kinetic data and in calculating pressure drop.

Pressure drop across the fluidised bed influences the sizing of the blower or compressor supplying the gas to the fluidised bed and is useful as an index of fluidised bed solids inventory.

Pressure drop in fixed bed has been studied extensively and the works of Blake, Burke and Plummer, Chilton and Colburn, Carman, Ergun and Leva are important. Ergun[9] proposed a generalised correlation:

$$\frac{\Delta P}{L} g_c = 150 \frac{(1-\epsilon)^2}{\epsilon^3} \frac{\mu u}{D_p^2} + 1.75 \frac{(1-\epsilon)}{\epsilon^3} \frac{Gu}{D_p} \qquad (1)$$

Where the first term Eq. (1) accounts primarily for the viscous energy losses, whereas the remaining term is primarily related to kinetic losses.

Leva et al[10] considered the incipient fluidising condition to be the extreme point in fixed bed conditions and attempted a correlation for Gmf in terms of the system properties, shape factor ϕ_s, and bed voidage at minimum fluidising conditions, ϵ_{mf}. Leva[11] modified the equation by expressing the unknowns ϕ_s and ϵ_{mf} as functions of R_e and gave an empirical correlation as

$$G_{mf} = 688\, D_p^{1.82} \left[\rho_f (\rho_s - \rho_f)\right]^{0.94} / \mu^{0.88} \qquad (2)$$

Where Gmf is in lb/ft^2/hr, Dp in inches, ρ in lb/cuft. and μ in centipoises. Based on a large volume of experimental data covering a wide variety of systems, Wen and Yu[8] developed empirical correlations. In this regard works of Miller and Logwinuk[12], van Heerden et al[13], Wilhelm and Kwauk[3] are significant.

Narasimhan[14], Pinchbeck and Popper[15], Goddard and Richardson[16] proposed correlations for predicting the minimum fluidizing velocity using the concept of free falling velocity.

Correlations for predicting minimum fluidising velocity based on drag force considerations have been attempted by Frantz[17], Ergun et al[18]., Pillai and Raja Rao[19] and Balakrishnan and Raja Rao[20]. Murthy and Raja Rao[21] attempted to measure G_{mf} and concluded that the only safe way to obtain G_{mf} is to measure it for individual gas-solid systems.

The pressure drop in a fluidised bed (ΔP) may be assumed to consist of the pressure drop due to the distributor and that due to the buoyant weight of the particles. The first factor is often small and the ΔP is taken equal to the apparent weight of the solids. This is frequently in error due to the inherent abnormalities present in a gas-solid fluidised bed namely channelling, bubbling and slugging. Adler and Happel[22] observed that the channelling tendencies arising from the preferential flow paths developed due to non-uniform voids or poor gas distribution severely reduced the ΔP and hence the particle fluid contact.

Bubbling is one of the inherent characteristics of any gas-solid fluidised system. The mechanics of the bubble formation, growth and rise velocity have been of considerable interest[23,24]. Davidson and Harrison[23] observed that the slug flow commences at an equivalent diameter of about 1/3 to 1/2 of the bed diameter. Hence it is important that to avoid bubbling, the distributor design should be proper and the bed height should be small.

Grohse[25] has shown that the quality of the bubbling fluidisation is strongly influenced by the type of the gas distributor. His finding may be summarised as follows:

For few air inlet openings, the bed density fluctuates appreciably. It is more severe at high gas velocity and gas channeling may be severe.

For many air inlet openings the fluctuation in the bed density is negligible at low flow rates and become appreciable at higher flow rates. Usually the bubbles are smaller and channeling is less.

Densely consolidated porous media or plates with many small orifices provide a superior contacting. But commercial scale operation with such distributors have a serious drawback of high pressure drop and hence high power consumption.

The hydrodynamic resistance of the grid must be of a certain magnitude if it is to distribute the fluidising medium evenly. The grid resistance depends on the rate of flow of the gas, but it may also be altered by means of number and also of apertures in the grid. The grid free area varies within the range of from 2 to 22%

of the total cross-sectional area of the grid. But grids with a free area higher than 50% have also been employed.

The following relation[26] for the fractional free area ensuring perfect mixing in the bed has been obtained from experiments with grids having free areas ranging from 2 to 10%.

$$a_r = 1.7 \left(\frac{u_p}{u_v}\right)^{0.9}$$

where a_r denotes the free area expressed as a % of the total grid area, and (u_p/u_v) is the ratio of the operating (u_p) and incipient fluidising velocity (u_v).

For holes from 5 to 10 mm in diameter, and for fractional free areas from 5 to 49%, the following empirical relation[27] is valid:

$$\Delta P_r = 1.44 \times 10^3 \left(\frac{u_p}{U_r}\right)^2$$

where ΔP_r is the grid pressure drop in kg/m², and u_p in m/sec.

The prediction of the bed expansion is necessary for specifying the height of the fluid bed equipment. Bed expansion has been studied by Matheson[28], Matheson et al[29], Davidson and Harrison[23]. Ramamurthy and Subba Raju[30] have obtained generalised equations for predicting bed expansion of annular liquid-fluidised beds by extending the equation of motion of a single particle in a fluid to a multiparticle system. They have also shown that the bed expansion characteristics, in annular spaces are not different from those tubes as long as the ratio of $D_{eq} / D_p > 8$.

<u>Baffles</u>

Baffles or other solid objects are usually employed in a fluidised bed (a) as diplegs, nozzles, probes, and structural members necessary for the proper operation of a process, (b) as horizontal or vertical tubes for heat exchange carrying, for example, steam or cooling water, (c) as objects immersed in the bed for processing, e.g. for drying, heating or coating, or (d) as obstacles fitted in the bed (i) to break up bubbles and so promote "smoother" fluidisation or (ii) to divide the fluidised bed unit into a number of stages in parallel or in series.

The effects of (a) on the behaviour of the fluidised system are rarely reported in the literature. The problems associated with (b), (c) and (d) have received much more attention. The majority of studies in the literature are concerned with cases (b) and (d) above.

A. <u>Horizontal Baffles</u> - Immersed horizontal tubes are a common feature of fluidised beds to which heat is supplied or removed. Two basic properties of the horizontal tube system that have been studied are (i) the flow pattern of particles and of fluidising fluid in the neighbourhood of the tubes, and (ii) the rates of bed/tube heat transfer. Glass and Harrison[31] have described a photographic investigation of the flow patterns of particles and of fluidising fluid near a horizontal tube in a fluidised bed. In the air-fluidised experiments, a tube was placed symmetrically about one quarter of the way up the particle bed from the distributor. They confirm that the particles circulate upwards near the sides of the tube and downwards further away; the circulation is smooth and continuous in the non-bubbling water-fluidised system, but bubbles in the air fluidised bed cause the circulation to be erratic and discontinuous.

Little systematic work has been done on the effect of an array of horizontal tubes on fluidisation behaviour. Glass[32] observed the effect of thirteen 1 cm diameter cylinders mounted in three horizontal rows on a 2 cm square pitch on the behaviour of a two dimensional air fluidised bed. The bubbles above the array were not noticeably different from those below it. This observation strongly suggests that unless the array of tubes almost fills the bed the influence it has on the average bubble size is small.

If heat transfer is to be good then the surface of heat exchange needs to be brought into contact as rapidly as possible with fresh particles from regions of the bed away from the surface. Therefore a defluidised region of the bed near a horizontal tube would be detrimental to good heat transfer and this indicates that the heat transfer to an object in a fluidised bed will be a function of the orientation of the object in the bed.

The broad conclusion from Morgan's work[33] is that at most fluidising flow rates slightly better heat transfer is obtained by arranging tubes vertically rather than horizontally. Horizontal tubes may also be preferred to vertical tubes at flow rates high enough to give rise to bubbles - or slugs - which envelope vertical tubes over most of their lengths.

Horizontal screens and Perforated Plates - When compared with an unbaffled bed, a bed containing horizontal screens or perforated plates has certain advantages, for example:
(i) Bubbles sizes tend to be smaller and fluidisation appears to be smoother (Emilio et al[34], Hall and Crumley[35]).
(ii) Gas-solids contacting is improved (Lewis et al[36]).
(iii) With a more uniform gas residence time, higher chemical conversions have been reported.

However, to set against these advantages solids mixing is impeded by the baffles (Baillie et al[34]), and so particles segregation can occur and it is difficult to fluidise all bed compartments simultaneously (Volk et al[37]).

D. Vertical Baffles - Vertical baffles in fluidised beds may be classified according to their shape and according to their size. Volk et al tested vertical baffles of various shapes including tubes, half-round sections, flat sections, and tubes with fins. However, none of the more complex geometries was found to be superior to the simple cylindrical shape. This is also the shape of vertical baffle which is simplest from a design stand point.

Vertical rods may be classified in two groups according to size (i) rods with diameter D_R big enough that they do not become enclosed by rising bubbles, for this condition to be met, $D_R/\bar{D}_O$ must be greater than about one-third and (ii) rods which are easily enclosed by rising bubbles, i.e. $D_R/\bar{D}_O$ less than about one-fifth. $\bar{D}_O$ is the diameter of the sphere having the mean bubble volume.

Sutherland[38] found that slugging was promoted by a single 7 cm diameter cylindrical insert in a 14 cm diameter bed. The approach to slugging conditions is accompanied by an increase in bed expansion (Volk et al[37]) and a decrease in heat transfer coefficient between the fluidised bed and the outer wall (Botterill[39]). The total amount of heat transferred may be increased , however, if the vertical rods are used as heat transfer surfaces.

Grace and Harrison[40] confirmed experimentally that vertical rods reduce the tendency of bubbles to coalesce obliquely and hence the development of non-uniformities of spatial bubble distribution is more gradual when thin vertical rods are present. Botton[41] showed that thin vertical rods cause a small reduction in bed expansion for beds of diameter less than 1m and an increase for larger beds.

Channeling Between Vertical Surfaces - If two surfacesare too close together, gas is drawn from the surrounding particulate phase into the gap between the surfaces where it rushes upwards at high velocity carrying widely dispersed particles thus establishing gas-channeling. To avoid this phenomenon Grace and Harrison[40] proposed that a distance of atleast thirty particle diameters should be maintained between all pairs of adjacent vertical surfaces in gas-fluidised beds.

Chemical Reactors with Vertical Baffles - Vertical rods which are too large to be enclosed by rising bubbles tend to promote slugging. A slugging fluidised bed has certain desirable features including good gas mixing characteristics and increased gas residence times (Hovmand and Davidson[42]) On the other hand, vertical rods which are enclosed by rising bubbles tend to occupy less space and to offer better surfaces for heat transfer. By reducing the size of bubbles and improving the uniformity of bubble distribution, such vertical rods lead to greater homogeneity with improved gas-solids contacting. Thus Hebden[43] found that a fluidised bed appeared to be 'pacified', by the addition of vertical rods and the carryover of particles was reduced.

Rowe and Stapleton[44] found that scaling-up fluidized beds from first principles present a complex problems. Volk etal [37] proposed a criterion of scale-up; that the equivalent bed diameter (free cross-sectional area/total wetted perimeter) be between 10 and 20 cm. For beds of diameter greater than 20 cm it was proposed that vertical rods be inserted in order to bring the equivalent bed diameter within the desired range. Chemical conversions in baffled beds were found to be as favourable as in open beds of the same equivalent diameter.

In view of the fact that the size of the vertical rod is an important variable in determining the behaviour of baffled fluidised beds, then the criterion of Volk et al. appears to be over simplified. The importance of the type of vertical baffle is underlined in that Agarwal and Davis[45] reached a conclusion which is contradictory to the Volk criterion, i.e., Agarwal and Davis, using vertical plates at regular intervals, proposed that small beds be baffled in order to simulate conditions in much larger beds, whereas Volk et al added cylindrical rods to large-scale beds to make their behaviour similar to the behaviour of small-scale fluidised beds.

One of the principal reasons for adding vertical surfaces to fluidised beds is to provide surfaces for heat transfer. In practice, vertical surfaces in fluidised beds may be associated with horizontal surfaces (e.g. Hardin[46]). Industrial processes where vertical baffles have been reported[37] include the Fisher-Tropsch synthesis, gas-making processes and the Hydrocol reaction and H-Iron reduction processes. In general, references to large units are few and this is without doubt because an effective baffle system for an industrial application has obvious commercial value, and so it is rarely reported in the literature.

Surfaces which are inclined both to the horizontal and to the vertical are seldom advantageous, because such surfaces encourage the channeling of gas on their under-sides and particle defluidization on their top-sides and both effects are detrimental to good gas-solids contacting and good bed-surface heat exchange.

It is not possible to specify a single type of baffle that is optimum for all possible applications, because each application of the fluidization technique depends for its success upon different properties of the bed to varying degrees. Vertical rods warrant consideration where heat transfer is of first importance.

CHAPTER III

EXPERIMENTAL SET-UP AND PROCEDURE

3.1 EXPERIMENTAL SET-UP

Flow patterns of fluid-solids contacting operations are conventionally indicated by observing the pressure drops across the bed as the fluid velocity through the bed is varied. Therefore, the apparatus constructed for these studies consisted essentially of a fluidising column to hold the solids bed and an arrangement to obtain pressure drop across the bed under different conditions of air-flow through the bed. The experimental set-up is shown schematically in Figure 3.1.

3.1.1 Overall Set-up of the Apparatus

Apparatus used in the present studies consisted of several perspex columns to hold the solids beds, rotameters to measure the airflow rates and a water manometer to indicate the pressure drops across the solids beds. A scale was attached along the entire length of the column to measure the heights of beds.

Compressed air at 6 kg/cm^2 was supplied by a compressor to a surge tank from which air was discharged at a controlled pressure of 1.5 kg/cm^2 and was also

3.2 PHYSICAL PROPERTIES OF MATERIALS

The three materials studied were spherical glass beads and crushed calcite and bauxite. Glass beads used were spherical in shape. Calcite and bauxite were crushed and ground to the desired particle sizes. Sieving of the products was done by a set of standard B.S. sieves. Size fractions of (-16+ 18) , (-22+25) and (-30 +40) mesh numbers were used. The arithmetic mean of the two appertures diameters of sieves designating the particular material fractions, was taken as the average particle size (B_p). The above mesh sizes correspond to an average diameter of 927 , 648 and 440 microns respectively.

Determination of solids density was carried out by liquid-displacement method. The liquids used were water and kerosene. The following were found to be the apparent density of the three materials bauxite, glass beads and calcite : 2.22 ,2.50 and 2.80 gm/cm^3 respectively.

3.3 EXPERIMENTAL PROCEDURE

3.3.1 Preparation of Solids Beds[47]

Wilhelm and Kwauk[3], Leva et al[10] and Miller and Logwinuk[12] have considerably contributed towards an understanding of flow patterns exhibited when fluid streams are passed through beds of finely divided solids.

It was recognised by Wilhelm and Kwauk that air-solid fluidisation experiments were more sensitive to the mode of bed preparation than the liquid-solid system. They performed their experiments 'under conditions of maximum and minimum consolidation." Maximum consolidation was achieved by tapping the column with a wooden mallet and the minimum by self settling after the bed was disturbed by passing a stream of air.

Leva et al and Miller and Logwinuk followed the latter procedure though none of these workers indicate why such methods for preparation of beds were followed. Data of Wilhelm and Kwauk and of Leva et al. On initial bed voidages indicate that they did not get uniform initial voidages for the same material and particle size, during the various runs.

On the other hand, Agarwal and Storrow[48] Baerg et al[18] and even Leva et al[49] have commenced their runs with solids beds obtained by just charging the materials into the columns. Oman and Watson[50] believed that much of the disagreement to be found among the earlier flow data on fluidised systems is due to the failure to prepare beds in a reproducible manner. It was, therefore, considered necessary to define the mode of bed preparation more precisely than had hitherto been by previous workers. Beds obtained by pouring uniformly sised materials into the column from a definite height and through a particular funnel opening were just fluidised and allowed to settle freely. Such beds attained under conditions of minimum consideration were found to be reproducible and were used in the present work.

MEASUREMENTS AND WORKING TECHNIQUES

Wilhelm and Kwauk[3], Leva et al [10] and many other workers studied the pressure drop and air-velocity relationships at increasing air velocities starting from a static or minimum consolidated bed, whereas Miller and Logwinuk[12] studied the phenomenon at increasing as well as decreasing velocities. The working procedure adopted in the present work is outlined below.

A known amount of solids, was poured into the column through a funnel provided at the top of the column. The bed was first fluidised and allowed to settle freely. Then the bed height was noted which was considered as the initial bed height. Air was passed through the bed at different rates by the control of air-inlet valve and the corresponding pressure drops across the bed as well as the bed heights were noted. The point at which there was a sudden drop in ΔP and particle movement seen, was noted as the minimum fluidizing condition and the corresponding mass flow rate was noted as G_{mf}.

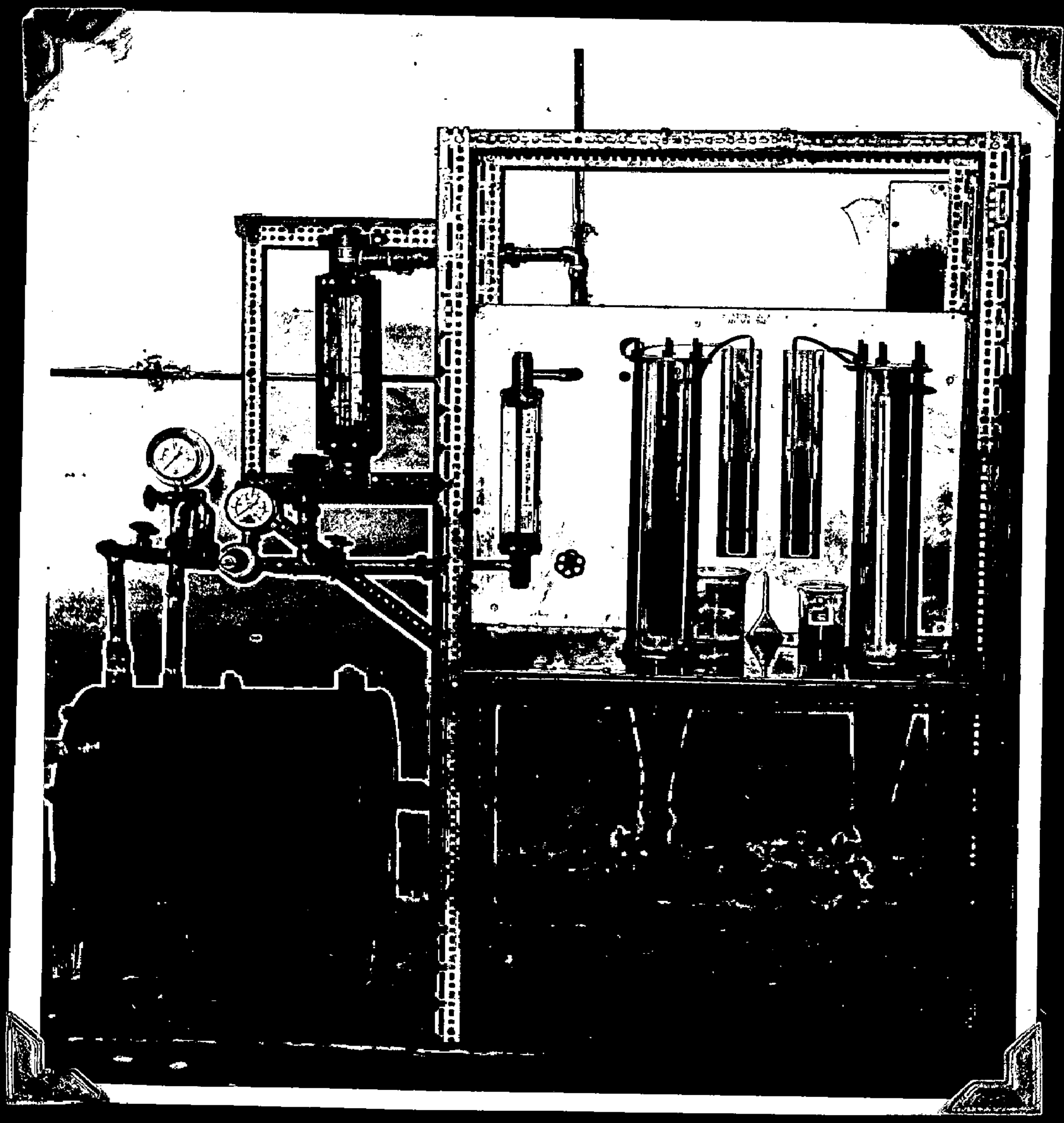

PLATE I. EXPERIMENTAL SETUP

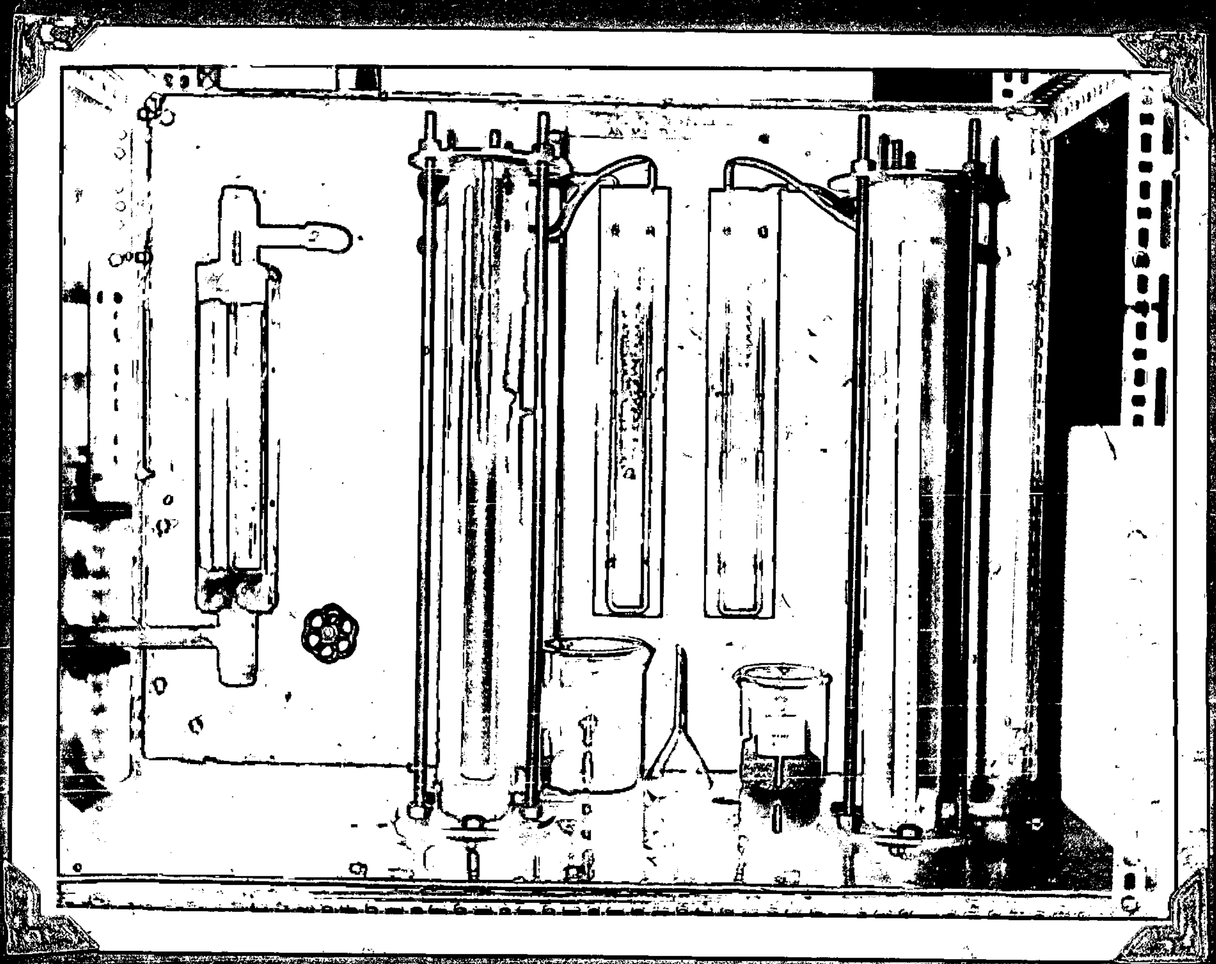

PLATE 2. FLUIDIZING COLUMNS

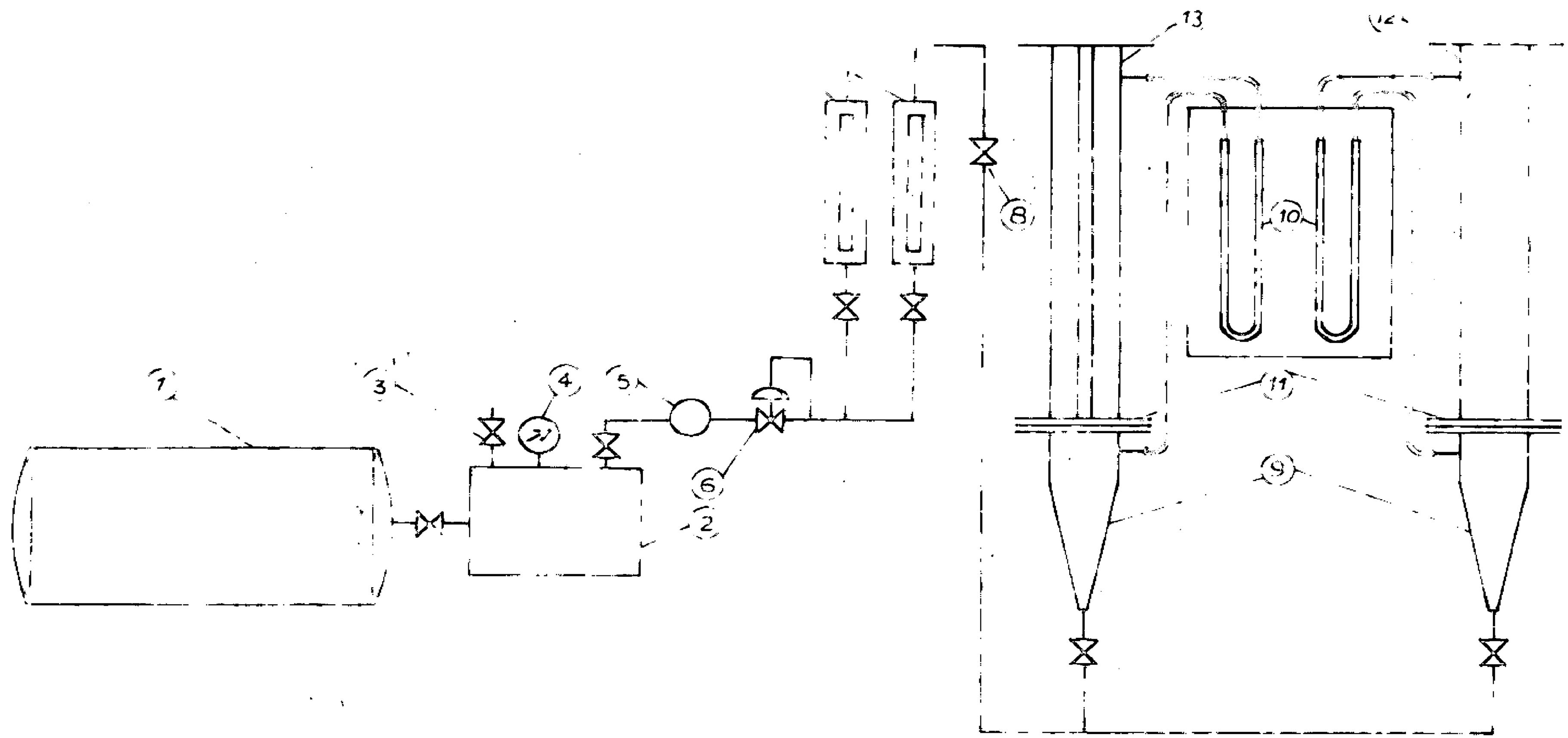

1 COMPRESSOR
2 SURGE TANK
3 VENT
4 PRESSURE GAUGE
5 AIR FILTER
6 PRESSURE REGULATOR
7 ROTAMETER
8 CONTROL VALVE
9 CALMING SECTION
10 MANOMETER
11 GRID PLATE
12 MAIN FLUIDIZING COLUMN (STRAIGHT TUBE)
13 MAIN FLUIDIZING COLUMN (ANNULUS)

FIG.3.1 SCHEMATIC DIAGRAM OF EXPERIMENTAL SET UP

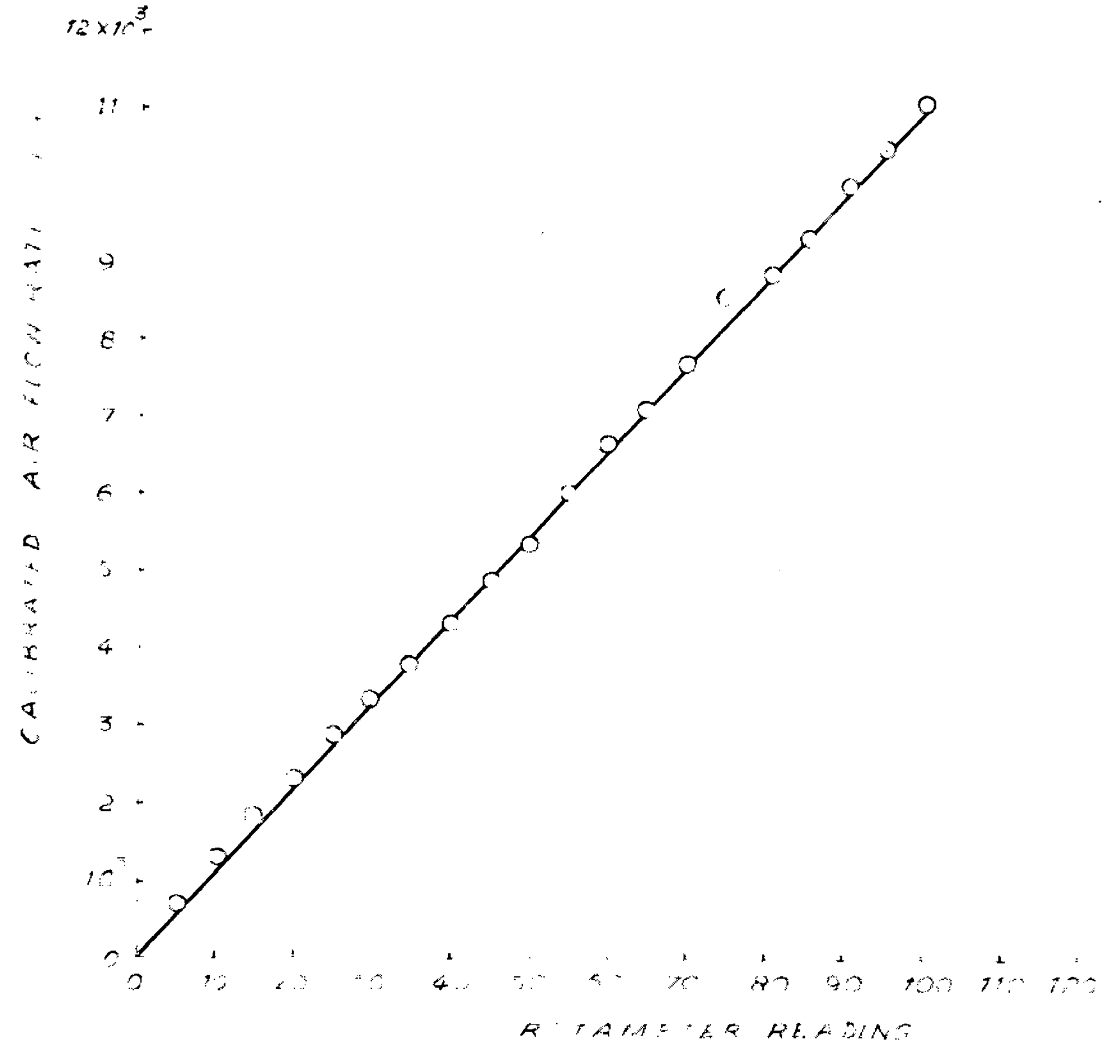

FIG. 3.2 CALIBRATION OF ROTAMETER

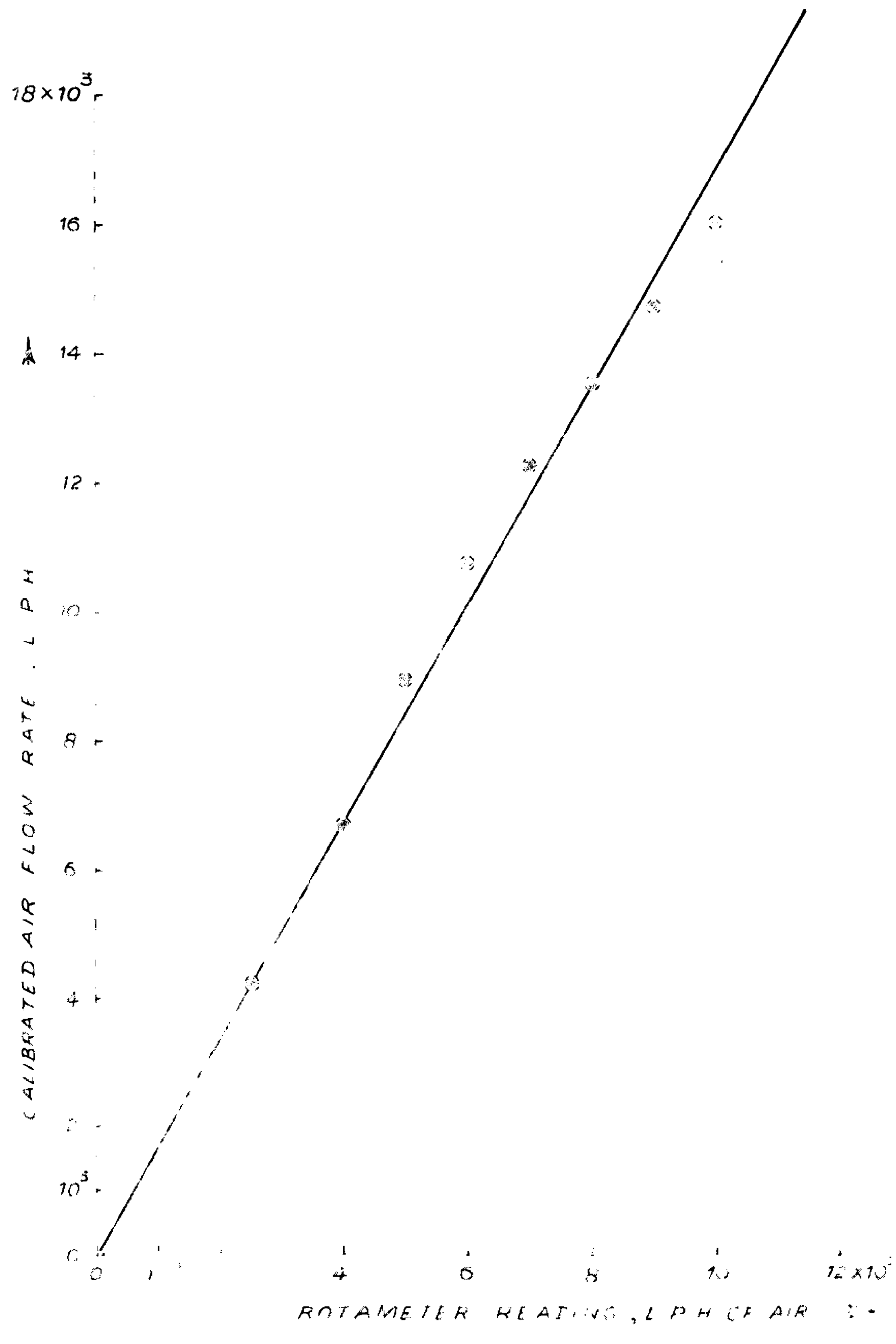

FIG.3.3 CALIBRATION OF ROTAMETER

CHAPTER IV

EXPERIMENTAL DATA AND OBSERVATIONS IN STRAIGHT TUBE

Experiments were conducted in straight cylindrical columns to obtain the relationship between air mass velocity and pressure drop across the bed of solids. Data were obtained in cylindrical perspex columns of i.d. 7, 5.7 and 5 cms for three materials viz., spherical glass beads, crushed calcite and bauxite of three different sizes and they are presented in Tables IV-1 to IV-3.

The studies in straight columns were conducted with an endeavour to compare the fluidisation behaviour with that in an annulus. To enable such a comparison, the ratio, weight of the bed per unit area of column cross-section i.e. W/A , was kept the same in both the cases .

The velocity pressure drop relationship obtained in these cylindrical columns is similar to that which has been established by many research workers. It was observed that only spherical glass beads resulted in smooth fluidisation. For larger sized particles, the G_{mf} required was higher.

In all the three columns, the observed G_{mf} values were greater than the values calculated using

Equation (2) proposed by Max Leva[11]. During the operation it was observed that only a part of the bed fluidised. The pressure drop recorded at this velocity was only due to the weight of that part of the bed supported by the rising stream of air. But at higher flow rates, a better distribution of air was observed.

In so far as the evidence of slugging is concerned , it was found to increase with increase in aspect ratio (L/D) . Slugging was less predominant in 7 cm. column. The crushed bauxite and calcite readily slugged whereas the spherical glass beads fluidised smoothly without any splashing and bumping. Slugging resulted in severe bed height and pressure drop fluctuations which made the observations more difficult.

TABLE IV.1

EXPERIMENTAL DATA - BATCH FLUIDIZATION IN STRAIGHT TUBE

COLUMN DIAMETER - 7.0 cm Material - Glass Beads (648 μ)

G_f gm/cm^{2}hr	ΔP gm/cm^2	L cm	G_f gm/cm^2 hr	ΔP gm/cm^2	L cm
1	2	3	1	2	3
Run No.1 , W =211 gms			Run No.2 W = 316.5 gms		
65.5	1.5	3.9	65.5	2.1	5.8
130	3.2	3.9	130	4.3	5.8
160	4.1	3.9	194	7.1	5.8
176	4.7	3.9	208	7.3	5.85
208	4.7	4.0	224	7.3	6.0
224	4.7	4.1	256	7.3	6.6
256	4.7	4.3	288	7.45	7.2
272	4.8	4.5	344	7.55	7.6
344	4.9	5.1	442	7.75	7.9
442	5.1	5.6	492	7.8	8.0
Run No.3 , W = 422 gms			Run No. 4 , W = 316.5 gms, (D_p = 927 μ)		
35	1.8	7.6	65.5	1.35	5.7
97.5	4.0	7.6	130.	2.9	5.7
160	7.4	7.6	194	4.7	5.7
211	10.65	7.6	240	6.0	5.7
224	10.1	7.7	260	7.5	5.7
256	10.1	8.2	272	7.3	5.7
320	10.1	9.3	304	7.3	5.8
393	10.3	10.0	344	7.3	6.0
442	10.4	10.5	393	7.4	6.3
492	10.6	11.5	442	7.6	7.3

p = 440 μ

1	2	3
Run No. 6, Bauxite		
35	3.3	8.0
50	4.5	8.0
81.5	7.1	8.0
97.5	7.4	8.1
113	7.2	8.4
45	7.2	9.3
76	7.2	10.2
24	7.4	10.7
56	7.55	11.5
20	7.7	13.5

TABLE IV.2

EXPERIMENTAL DATA - BATCH FLUIDIZATION IN STRAIGHT TUBE

Column Diameter = 5.0 cm. Material - Glass beads (648 μ)

G_f gm/cm^{2}hr	ΔP gm/cm^2	L cm.	G_f gm/cm^2 hr	ΔP gm/cm^2	L cm
1	2	3	1	2	3
Run No. 8, W = 65.43 gms			Run No. 9, W = 130.86 gms.		
98.4	1.2	2.0	37	1.0	5.2
160	2.4	2.0	98.4	2.4	4.2
191	2.8	2.0	160	4.0	4.2
197	2.8	2.0	222	5.9	4.2
254	2.8	2.2	250	5.85	4.3
345	3.0	2.7	254	5.9	4.4
502	3.2	3.4	314	6.0	4.9
627	3.4	4.0	379	6.1	5.8
770	3.6	4.4	439	6.2	6.1
866	3.8	5.9	627	6.4	6.8
Run No.10, W= 196.3 gms			Run No. 11, W = 261.72 gm.		
68.4	2.6	6.3	68.4	2.8	8.4
128.3	4.5	6.3	128.3	5.3	8.4
191	6.6	6.3	191	2.9	8.4
254	9.0	6.4	254	10.8	8.4
285	9.0	6.7	291	12.4	8.5
314	9.0	7.1	314	12.4	9.1
379	9.2	8.4	379	12.4	10.6
502	9.4	10.0	439	12.6	12.4
565	9.55	11.1	6.65	13.0	15.0
627	9.7	12.2	627	13.2	16.0

Table IV.2(Contd..)

Weight of Charge = 196.3 gms

1	2	3	1	2	3
Run No. 12, Glass beads(440µ)			Run No.13 Bauxite (927 µ)		
37	1.9	6.4	68.4	1.5	9.0
98.4	4.5	6.4	160	3.9	9.0
160	7.35	6.4	254	6.0	9.0
191	8.9	6.4	325	9.4	9.5
202	8.8	6.8	341	9.3	9.8
222.5	8.8	6.9	345	9.3	10.4
254	9.0	7.4	360	9.3	11.4
314	9.2	8.5	379	9.3	12.2
379	9.4	9.0	470	9.6	13.0
439	9.6	9.7	502	9.7	14.2
Run No.14, Bauxite (648 µ)			Run No.15, Bauxite (440 µ)		
68.4	2.3	8.9	37	2.7	9.0
128.3	4.7	8.9	98.4	6.3	9.0
191	6.9	8.9	160	9.2	9.4
254	9.7	8.9	171	9.3	9.7
260	9.2	9.2	191	9.3	10.5
285	9.2	9.8	222.5	9.3	11.9
314	9.2	11.0	254	9.3	12.6
379	9.4	12.8	314	9.5	14.5
439	9.7	15.2	345	9.6	16.0
502	9.9	16.8	408	9.6	16.0

Table IV.2 (Contd...)

Weight of Charge = 196.3 gms

1	2	3	1	2	3
68.4	3.9	6.5	128.3	2.9	7.7
128.3	7.5	6.5	254	6.3	7.7
185	9.3	7.1	314	8.4	7.7
191	9.2	7.1	365	9.3	8.1
254	9.2	8.3	379	9.2	8.3
285	9.2	9.1	408	9.2	8.8
345	9.2	10.5	470	9.2	10.1
408	9.4	11.6	533	9.4	11.7
470	9.6	11.8	565	9.5	12.0
502	9.7	12.0	627	9.7	12.6
Run No. 16, Calcite(440 μ)			Run No. 17, Calcite (927 μ)		

TABLE IV-3

EXPERIMENTAL DATA - BATCH FLUIDIZATION IN STRAIGHT TUBE

Column Dia . 5.7 cm, Material - Glass Beads (648 μ)

G_f gm/cm^{2}hr	ΔP gm/cm^2	L cm	G_f gm/cm^{2}hr	ΔP gm/cm^2	L cm
1	2	3	1	2	3
Run No. 18, W=110.5 gm			Run No. 19, W = 221.0 gm.		
71.5	1.6	3.1	52.9	1.8	6.1
147.5	3.1	3.1	147.5	4.5	6.1
185	4.1	3.1	222	7.4	6.1
189	3.9	3.15	238	8.5	6.1
196	3.9	3.15	242	8.1	6.3
242	3.9	3.4	293	8.1	6.6
293	3.9	4.0	339	8.1	7.7
339	4.0	4.4	436	8.3	8.6
594	4.3	6.0	594	8.55	9.4
734	4.5	6.3	734	8.75	9.6
Run No. 20, W = 331.5 gm			Run No. 21, W = 442 gm		
99	3.7	9.2	99	4.5	12.3
147.5	5.7	9.2	147.5	6.5	12.3
196	8.85	9.2	196	9.6	12.3
242	10.5	9.2	242	12.3	12.3
270	12.3	9.2	304	16.75	12.3
282	12.1	9.4	308	16.6	12.8
293	12.1	9.5	324	16.6	13.
314	12.3	10	363	16.9	14.1
366	12.6	11.2	436	17.4	15.4
484	13.0	13.0	594	18.3	17.0

Table IV.3 (Contd..)

Weight of charge = 331.5 gm

1	2	3	1	2	3
Run No. 22 , Glass beads(927 μ)			Run No. 23, Glass beads(440 μ)		
52.8	1.8	9.0	28.6	1.8	9.1
147.5	4.9	9.0	71.5	4.0	9.1
242	9.35	9.0	123	6.8	9.1
293	11.8	9.0	171.7	10.0	9.1
314	12.85	9.1	207	12.7	9.2
319	12.7	9.2	222	12.3	9.4
339	12.7	9.5	246.5	12.3	10.2
363	12.7	10	268	12.3	10.6
436	13.0	12	314	12.6	11.6
560	13.4	13.5	436	13.1	13.8
Run No. 24, Bauxite (927 μ)			Run No. 25, Bauxite (648 μ)		
52.8	1.9	12.2	52.8	3.05	12.3
147.5	5.2	12.2	99	5.3	12.3
227	8.7	12.2	147.5	8.5	12.3
268	11.5	12.2	196	11.6	12.3
295	12.5	12.5	222	12.6	12.4
304	12.6	12.6	236	12.6	13.1
308	12.6	12.8	242	12.6	13.6
319	12.6	13.4	268	12.8	14.7
387	12.9	15.4	314	13.1	17.7
436	13.8	18.3	387	13.9	20.0

Table IV.3 (Contd...)

Weight of Charge 331.5 gm

1	2	3	1	2	3
Run No. 26 Bauxite (440 μ)			Run No. 27 Calcite (440 μ)		
52.8	5.8	12.2	52.8	4.3	9.4
71.5	7.7	12.2	99	7.6	8.4
99	10.2	12.2	147.5	11.9	9.4
123	12.7	12.2	174	12.7	10
134	12.4	13	196	12.5	10.7
147.5	12.75	13.2	222	12.5	11.5
160.5	12.7	14.1	268	12.5	13
196	12.9	16.2	314	12.7	14.8
242	13.3	17.9	387	13.2	15.0
293	14.0	20	436	13.5	15.3

TABLE IV.4

EXPERIMENTAL AND CALCULATED VALUES OF G_{mf} AND ΔP_{mf} IN STRAIGHT TUBE

Material	D_p microns	D_t/D_p	G_{mf} Obs. gm/cm² hr	G_{mf} Leva gm/cm² hr	ΔP_{mf} Obs. gm/cm²	Δr
		D_L = 7 cm , W/A = 8.22 gm/cm²				
Glass beads	927	75.5	272	262	7.3	0.890
Glass beads	648	108	208	137	7.3	0.890
Bauxite	440	159	113	64	7.2	0.875
Glass beads	440	159	142	68.7	7.1	0.865
Calcite	440	159	122	77	7.4	0.900
		D_L = 5 cm, W/A = 10 gm/cm²				
Bauxite	927	54	341	244	9.3	0.930
Bauxite	648	77	260	127	9.2	0.920
Glass beads	648	77	254	137	9.2	0.920
Bauxite	440	114	171	64	9.3	0.900
Glass beads	440	114	202	68.7	8.8	0.880
Calcite	440	114	191	77	9.3	0.930
		D_L = 5.7 cm , W/A = 12.96 gm/cm²				
Bauxite	927	61.5	304	244	12.6	0.972
Glass beads	927	61.5	319	262	12.7	0.980
Bauxite	648	88	222	127	12.6	0.972
Glass beads	648	88	282	137	12.1	0.935
Bauxite	440	130	134	64	12.4	0.956
Glass beads	440	130	222	68.7	12.3	0.950
Calcite	440	130	196	77	12.5	0.965

CHAPTER V

EXPERIMENTAL DATA AND OBSERVATIONS IN ANNULUS

Pressure drop studies were carried out in three annuli. In all the three cases, the i.d. of the outer tube was 7 cm . Perspex tubes of 1.58, 3.27 and 4.42 cm o.d. were employed as the inner tubes and the equivalent diameter of each annulus is 5.42 , 3.73 and 2.58 cms respectively. Fluidisation behaviour of three materials viz. glass beads, calcite and bauxite of three different sizes viz., 927, 648 and 440 microns was studied. The bed weight was 300 gm in all the cases.

Experimental data are presented in Tables V.1 to V.3 , and the experimental observations can be summarised as follows .

As the air velocity through the bed was increased the variation in pressure drop across the bed also increased Under these conditions the solids were in a fixed bed, the air channeling through the interstices between particles, without any motion of the particles. At a still higher velocity, the bed expanded slightly and then only a part of the bed was fluidized. The pressure drop measured across the bed was less than the weight of the bed per unit area of cross section. With a still increase in air flow rate, beyond the onset condition, the air distribution was better and the other parts of the bed, which were inert, to start with, also started fluidizing. The pressure drop remained almost constant over a certain range of air flow rate beyond G_{mf} after which it gradually increased in certain cases due to slugging.

The quality of fluidization in the annulus with a cross-sectional area of 36.55 cm^2, was found to be better when compared with that in the other two annuli with area of cross section 30 and 23.15 cm^2. Slugging, to a great extent, was absent and the fluctuations in, pressure drop and bed height were comparatively reduced. The annulus with 30 cm^2 area of cross section behaved very similar to the annulus with 36.55 cm^2 area of cross section. Channeling was observed in 36.55 cm^2 annulus. For larger sized particles, the bed slugged at a flow rate just higher than G_{mf} whereas the finer particles fluidized smoothly even at high flow rates beyond the minimum fluidizing velocity.

TABLE V.1

EXPERIMENTAL DATA - BATCH FLUIDIZATION IN ANNULUS

Column Dia. D_2 = 7 cm, D_1 = 1.58 cm, Material = Glass beads(648μ)

G_f gm/cm^2 hr	ΔP gm/cm^2	L cm	G_f gm/cm^{2}hr	ΔP gm/cm^2	L cm
1	2	3	4	2	3
Run No. 28, W= 200 gms			Run No.29, W = 300 gms		
36.7	1.3	3.8	36.7	1.85	5.8
85.6	2.7	3.8	68.8	3.4	5.8
119.5	3.9	3.8	102.5	5.1	5.8
153	5.0	3.8	144	7.7	5.8
162	4.9	3.85	147	7.4	6.0
185	4.9	3.9	153	7.4	6.0
236	4.9	4.3	168.5	7.4	6.1
256	5.0	4.4	204	7.4	6.3
336	5.2	5.3	270	7.6	6.8
517	5.4	6.3	465	7.8	7.9
Run No. 30, W = 400 gm			Run No. 31, W = 300 gms Glass beads (927 μ)		
68.8	4.6	7.5	102.5	3.6	5.6
136	9.2	7.5	168.5	4.6	5.6
153	10.2	7.5	219.	6.8	5.6
154.5	10.4	7.6	249	7.9	5.6
159	10.2	7.6	256	7.6	5.6
185	10.20	8.0	270	7.6	5.65
270	10.2	8.8	303	7.6	6.1
3.03	10.3	9.0	336	7.6	6.4
413	10.5	9.5	413	7.8	6.9
517	10.7	10.4	517	8.0	7.2

Table V.1 (Contd..)

Weight of charge 300 gms.

1	2	3	1	2	3
Run No. 32 , Glass beads (440 μ)			Run No. 33, Bauxite (440μ)		
52.8	3.6	5.7	36.7	4.6	7.5
85.6	5.7	5.7	61	7.4	7.5
119.5	7.9	5.7	68.8	7.8	7.7
121	7.4	5.75	70.5	7.4	7.9
136	7.4	5.8	102.5	7.4	8.8
168.5	7.4	6.2	168.5	7.4	9.6
185	7.55	6.5	236	7.4	10.5
236	7.70	6.8	270	7.5	11.0
413	7.9	7.8	303	7.6	11.4
465	8.0	8.0	336	7.7	11.6
Run No. 3 4 , Calcite (440 μ)			Run No. 35 , Bauxite (648 μ)		
52.8	4.6	5.7	36.7	2	7.6
68.8	6.0	5.7	68.8	3.6	7.6
95	7.8	5.7	103.	5.5	7.6
98	7.4	5.9	150	7.9	7.6
119.5	7.4	6.5	15 3	7.5	7.8
168.5	7.4	6.9	168.5	7.5	8.0
236	7.4	7.3	204	7.5	8.5
270	7.5	7.6	270	7.5	9.0
303	7.6	8.0	303	7.6	9.7
413	7.8	8.8	336	7.7	10.0

TABLE V.2

EXPERIMENTAL DATA - BATCH FLUIDIZATION IN ANNULUS

Column Dia , D_2 = 7 cms, D_1 = 3.27 cm, Material Glass beads (648 μ)

G_f gm/cm²hr	ΔP gm/cm²	L cm	G_f gm/cm²hr	ΔP gm/cm²	L cm
1	2	3	1	2	3
Run No. 36, W = 100 gms			Run No. 37, W = 200 gms.		
44.7	1.1	1.9	64.4	2.4	3.9
84	2	1.9	104.5	4.2	3.9
125	2.95	2	145.5	6.1	4.1
128.5	3.1	2.1	149	5.9	4.3
136	3.1	2.1	166	6.05	4.5
145.5	3.1	2.2	205	6.5	4.8
186.5	3.4	2.4	248	6.9	5.0
248	3.8	2.7	287.5	7.1	5.3
369	4.7	3.1	369	7.8	6.0
440	5.3	3.9	566	9.8	7.9
Run No. 38, W = 300 gms			Run No. 39, W = 400 gms.		
44.7	2.7	6.0	44.7	3.5	8.3
84	4.9	6.0	84	6.35	8.3
125	7.6	6.1	125	9.5	8.3
158	9.3	6.4	166	12.75	8.7
162	9.2	6.6	173.5	12.2	9
186.5	9.2	6.9	186.5	12.2	9.2
205	9.3	7.3	248	12.6	10
248	9.7	7.7	369	13.7	12.6
328	10.4	9.0	504	15.1	15.0
410	11.2	11.1	630	16.3	16.3

Table V.2(Contd..)

Weight of charge W = 300 gms.

1	2	3	1	2	3
Run No. 40, Glass beads (440 μ)			Run No. 41, Bauxite (4927 μ)		
44.7	4.4	6.3	44.7	1.8	8.8
84	7.8	6.3	104.5	4.1	8.8
108.1	8.5	6.8	166	7.1	8.9
125	8.5	7.3	205	9.8	8.9
166	8.5	8.4	218	9.5	9.1
186.5	8.6	8.9	226	9.5	9.3
248	9.0	10.4	248	9.5	9.8
328	9.5	11.7	280.5	9.9	10.7
440	10.1	12.7	349	10.5	12.6
630	10.9	13.6	440	11.6	15.2
Run No. 42, Bauxite(648μ)			Run No. 43 Bauxite (440 μ)		
64.4	4.6	8.5	24	5.2	8.5
104.5	7.6	8.5	37	7.0	8.5
125	9.3	8.5	52.0	9.0	8.7
136	9.0	9.0	64.4	8.5	9.3
145.5	9.0	9.2	104.5	8.5	10.3
166	9.0	9.5	125	9.0	10.7
205	9.2	10.4	187	9.6	12.4
287.5	10.2	12.5	226	10	14.4
369	11	14.8	288	10.5	16.9
440	12	17.	349	11	20.

Table V.2 (Contd...)

Weight of charge , W = 300 gm

1	2	3	1	2	3
Run No. 44, Calcite (440 μ)			Run No. 45, Calcite (927 μ)		
24	3.2	6.3	44.7	1.6	7.7
64	7.0	6.3	104.5	3.6	7.7
88	8.9	6.9	125	4.6	7.7
104.5	8.6	7.2	166	6.2	7.7
125	8.6	7.4	205	8.4	7.7
145.5	8.8	7.6	248	10	7.9
187	9.2	8.1	259	9.7	8.1
226	9.6	8.8	287.5	10	8.4
308	10.4	11	369	10.6	10
410	11 .5	13.5	504	12.1	13
Run No. 46, Glass beads (927 μ)					
64.4	2.6	6.2			
104.5	4.2	6.2			
145.5	6.4	6.2			
205	8.8	6.5			
22 6	9.6	6.5			
248	9.8	6.8			
267	10	7.1			
328	10.6	8.4			
369	11	9			
410	11.4	10			

TABLE V.3

EXPERIMENTAL DATA - BATCH FLUIDIZATION IN ANNULUS

Column Dia. D_2 = 7 cm, D_2 = 4.42 cm, Material - Glass beads (648 μ)

G_f gm/cm^{2}hr	ΔP gm/cm^2	L cm.	G_f gm/cm^{2}hr	ΔP gm/cm^2	L cm
1	2	3	1	2	3
Run No. 47, W = 100 gm			Run No. 48, W = 200 gm.		
109	2.2	2.4	58	2	5.4
162	3.5	2.4	109	3.6	5.3
189	3.7	2.7	163	5.6	5.4
216	3.7	2.8	216	8.2	5.4
243	3.7	3.0	218	7.5	5.8
294	3.7	3.3	243	7.5	6.1
347	4.0	3.5	267	7.5	6.7
480	4.3	4.6	400	7.7	8.7
615	4.6	5.3	534	8.2	9.5
820	5.0	5.6	820	9.0	10.0
Run No. 49, W = 300 gm			Run No. 50, W = 400 gm.		
83	3.7	8.3	58	3.3	11.4
162	7.5	8.3	162	9.1	11.4
216	10.5	8.3	218	13.3	11.4
250	12.7	8.5	243	15.0	11.4
257	11.2	9.4	267	17.1	11.5
267	11.2	9.6	276	16.0	13.0
294	11.2	10.0	294	16.0	13.8
347	11.6	11.0	347	16.0	14.9
480	12.0	12.4	427	16.8	16.0
655	12.4	13.2	534	17.5	17.5

Table V.3 (Contd...)

Weight of charge , = 300 gms.

1	2	3	1	2	3
Run No. 51, Glass beads (927 μ)			Run No. 52 , Glass beads(440 μ)		
109	3.0	8.6	32	2.5	8.3
162	4.8	8.6	84	6.0	8.3
267	9.0	8.6	136	9.9	8.3
322	11.4	8.6	162	11.9	8.3
349	13.0	8.8	165	12.2	8.4
356	12.2	9.2	170	11.5	8.8
427	11.9	10.5	243	11.2	11
480	12.2	11.3	322	11.5	12.8
655	12.8	12.4	427	11.8	14.3
820	13.4	13.0	480	12.0	15.0
Run No. 53, Bauxite (927 μ)			Run No. 54, Bauxite (648 μ)		
109	4.0	11.5	58	3.1	11.3
162	6.1	11.5	109	5.7	11.3
216	8.5	11.5	162	9.0	11.3
267	11.2	11.6	189	10.9	11.3
295	12.8	11.7	204	12.0	11.3
322	13.7	12.2	228	13.0	11.7
325	11.8	13.2	234	12.0	12.6
347	11.8	14.3	245	12.0	13.5
427	12.1	15.9	374	12.0	16.1
534	12.6	17.5	480	12.5	18.6

Table V.3 (Contd...)

Weight of Charges = 300 gm.

1	2	3	1	2	3
Run No. 55, Bauxite (440 μ)			Run No. 56, Calcite (440 μ)		
31	3.1	11.0	31	3.2	8.5
58	5.7	11.0	58	6.1	8.5
84	8.3	11.0	84	8.1	8.5
109	11.0	11.0	128	11.9	8.5
121	12.4	11.4	138.5	11.7	9.0
136	13.2	11.4	162	11.0	10.3
138.5	11.5	12.3	189	10.8	11.0
162	11.0	13.5	267	11.0	13.0
243	10.4	16.7	374	11.5	13.9
322	11.0	18.1	427	11.9	14.5

TABLE V.4

EXPERIMENTAL AND CALCULATED VALUES OF G_{mf} AND ΔP_{mf} IN ANNULUS

Material	D_p microns	D_A/D_p	G_{mf} Obs. gm/cm^2hr	G_{mf} Leva gm/cm^2hr	ΔP_{mf} Obs. gm/cm^2	Δw
$D_2 = 7$ cm, $D_1 = 1.58$ cm, $W/A = 8.22\ gm/cm^2$						
Bauxite	927	29.2	226	244	7.5	0.914
Glass beads	927	29.2	2[illegible]6	262	7.6	0.925
Bauxite	648	41.8	153	127	7.5	0.914
Glass beads	648	41.8	147	137	7.4	0.900
Bauxite	440	61.5	70.5	64	7.4	0.900
Glass beads	440	61.5	121	68.7	7.4	0.900
Calcite	440	61.5	98	77	7.4	0.900
$D_2 = 7$ cm, $D_1 = 3.27$ cm, $W/A = 10\ gm/cm^2$						
Bauxite	927	20.1	218	244	9.5	0.95
Glass bead s	927	20.1	226	262	9.6	0.96
Bauxite	648	28.8	136	127	9.0	0.90
Glass beads	648	28.8	162	137	9.2	0.82
Bauxite	440	42.4	6[illegible].4	64	8.5	0.85
Glass beads	440	42.4	108.1	68.7	8.5	0.85
Calcite	440	42.4	104.5	77	8.6	0.86
$D_2 = 7$ cm, $D_1 = 4.42$ cm, $W/A = 12.96\ gm/cm^2$						
Bauxite	927	13.9	325	244	11.8	0.913
Glass beads	927	13.9	356	262	12.2	0.943
Bauxite	648	19.9	234	127	12.0	0.927
Glass beads	648	19.9	257	137	11.2	0.865
Bauxite	440	29.4	138.5	64	11.5	0.89
Glass beads	440	29.4	170	68.7	11.5	0.89
Calcite	440	29.4	138.5	77	11.7	0.905

CHAPTER VI

RESULTS AND DISCUSSIONS

6.1 COMPARISON OF FLUIDIZATION IN ANNULUS WITH THAT IN STRAIGHT TUBE

The pressure drop flow diagrams for the three materials viz., spherical glass beads, crushed calcite and bauxite were obtained in straight tube and annulus, keeping the weight of the bed per unit cross-sectional area of the column i.e., W/A , same in both cases. Samples of primary data collected during the various experimental runs are graphically presented in Fig. 6.1 to 6.5. From such representations ΔP across a solids bed and G_{mf} were determined.

It was observed that for the same solids loading, per unit cross sectional area of the column , the ΔP experienced in annulus was higher compared to that in straight tube. Particle position is only a function of time in an ideal batch fluidised bed and is independent of the geometry of the vessel. But in an annulus the presence of the internal tube restricts the free space available for the movement of solids. Hence the position of a solid particle gets affected by D_A/D_p ratio. It is expected that lower is the D_A/D_p ratio, greater will be the resistance to free solids movement. This is reflected in the higher ΔP in annulus.

The G_{mf} observed in annulus was lower than that in straight tube. For a particular velocity of air, ΔP was more in annulus and hence lesser air velocity was required to reach the onset of fludiza-tion condition.

In both annulus and straight tube, at the reported incipient fluidizing condition, only a part of the bed was supported by the rising stream of air and hence the ΔP measured at that condition was lower than the theoretical value , W/A. This is clearly an indication of 'channeling'.

6.2 EFFECT OF BED WEIGHT

The pressure drop flow diagrams for four wei-ghts viz., 100, 200, 300 and 400 gm of glass beads (648 μ) in the three annuli are given in Fig. 6.6, 6.7, and 6.8 . Data presented in Tables IV.1, IV.2, and IV.3 of experiments in 36.55 and 30.00 cm^2 annular columns indicate that variations in bed weights cause negligible variations in G_{mf} values. On the other hand, in a 23.15 cm^2 column, onset of fluidization was observed to set in at increasingly higher velocities with increases in bed weight. Such an observation points to the fact that in the case of 23.15 cm^2 column , at the incipient bubbling conditions, increased energy requirements provided by higher gas velocities are needed for the conversion of a fixed bed into a fluidized one. Thus it appears, the wall effect with respect to incipient fluidization conditions is to a great extent dependent on the D_A/D_p ratio.

6.3 EFFECT OF PARTICLE SIZE (D_p)

The pressure drop flow diagrams with D_p as the parameter are presented in Fig. 6.9 to 6.11. It is inferred that a larger sized particle required a higher G_{mf} This is in complete accordance with the earlier findings. But on the other hand a smaller sized particle yielded a higher ΔP since the specific surface, i.e. surface per unit volume or weight, increases as particle size decreases. Hence inter-particle friction is higher for a smaller sized particle which leads to higher ΔP.

6.4 EFFECT OF ANNULUS SIZE

Sample pressure drop flow diagrams with annulus size as the parameter for glass beads, bauxite and calcite are presented in Fig. 6.12 to 6.14. For a particular material and size, G_{mf} required in the annular columns with a cross-sectional area of 36.55 and

30.00 cm^2 was nearly the same. But for the 23.15 cm^2 column the G_{mf} required was higher. D_A/D_p was comparatively smaller for 23.15 cm^2 annulus and hence the particle movement was considerably impeded, warranting a higher velocity to 'unlock ' and bring the solids bed to the state of incipient fluidization. Beyond the onset of fluidization, slugging occurred readily in 23.15 cm^2 column and the entire bed was seen to bump and splash resulting in severe fluctuations in bed height and pressure drop. The 36.55 cm^2 column was observed to yield a smoother fluidization compared to the remaining two though it exhibited channeling tendencies to a certain extent.

6.5 MINIMUM FLUIDIZING VELOCITIES (G_{mf})

G_{mf} values were determined for the three materials in both cylindrical and annular batch fluidisers. The equipment used was described in Chapter III and the experimental procedure followed was given in the same chapter. Materials employed in determining G_{mf} were spherical glass beads, crushed calcite and bauxite with a D_p of 927, 648 and 440 microns.

The experimental and calculated values of G_{mf} in straight tube and annulus are given in Tables IV-4 and V-4 respectively.

G_{mf} values were calculated for annulus using different materials by Max Leva's equation which is presented by Eqn (2) in Chapter II. It is noticed that the calculated values of G_{mf} were very much different from the observed values. Leva's equation predicts the G_{mf} values satisfactorily for straight tubes. It would be easier to predict the G_{mf} value for annulus using Leva's equation with a correction factor to account for the difference between a straight tube and annulus.

In an annulus the particle movement is governed by the free radial distance (expressed as D_A/D_p) and the peripheral path (expressed as A_1/A_2). For the same outer tube, different inner tubes will give different D_A/D_p ratios and A_1/A_2 ratios.

Larger is the annulus, easier will be the particle movement and the observed G_{mf} will be closer to the predicted values using Leva's equation. Smaller is the annulus, the observed values will be far away from the predicted values. As the annulus size becomes larger particularly when the inner tube diameter is smaller, the G_{mf} values observed, may approach the predicted values by Leva's equation. So a correlation has been proposed for predicting the G_{mf} in annulus as ($\frac{G_{mf\ X}}{G_{mf\ Leva}}$) in terms of D_A/D_p and A_1/A_2.

The proposed correlation is as follows :

$$\left[\frac{G_{mf\ A}}{G_{mf\ Leva}}\right] = 0.12 \left(\frac{D_A}{D_p}\right)^{0.55} \left(\frac{A_1}{A_2}\right)^{-1.90}$$

The above correlation was obtained on the basis of a regression analysis so that the equation gave minimum deviation from the observed values. Fig. 7.1 shows a plot of observed versus correl ated values of $\left[\frac{G_{mf\ A}}{G_{mf\ Leva}}\right]$ and the variation of 85 % of the observed values in comparison with the predicted values lies within ± 16.4 %.

6.6 PRESSURE DROP AT THE ONSET OF FLUIDIZATION (ΔP_{mf})

Additional light is shed on the nature of fluidised beds by examining the dimensionless pressure drop across the bed. The latter is defined as the ratio of the ΔP_{mf} to the weight of the bed per unit area of cross section or

$$\Delta W = \frac{\Delta P_{mf}}{(W/A)}$$

ΔW was affected to a certain extent by the settled bed depth or quantity of material. For instance, in the 36.55 cm^2 annulus, the ΔW increased from 0.895 to 0.931 as the settled bed depth was raised from

3.8 to 7.5 cms. These results indicate that more of the weight of the bed was supported by rising gas in deeper beds than in shallower beds. This provided further evidence that deeper beds more nearly approach normal fluidisation than in shallower ones.

Table V.4 gives the ΔW values obtained at various operating conditions. For ideal fluidised beds ΔW approaches unity. A scrutiny of the tabulated results shows that ΔW is invariably less than unity for the three materials studied. Hence the bed of material was not supported fully by the rising flow of gas and it must have been supported, in part, by the grid plate or the walls. This finding seems to indicate that the bed had more structure and was less fluid-like than a normal fluidised bed. The exiBtence of stagnant, or at least semi-stagnant areas, were confirmed by visual observations.

The lower-than-theoretical values for ΔP may be due to channeling which is quite likely to occur when a multi-orifice plate gas distributor is used. This explanation is in agreement with that offered by Lewis et al[36]. But channeling tendency was observed to be reduced considerably at higher flow rates due to higher solids circulation.

An equation to predict ΔP_{mf} in an annulus is proposed of the form

$$\Delta P_{mf} = k \left[\frac{W}{A}\right] \left[\frac{D_A}{D_p}\right]^a \left[Re_{mf}\right]^b$$

At the minimum fluidising velocity, particles are suspended. For a particle to be freely suspended energy requirement will depend upon resistance to free movement i.e. D_A/D_p ratio. In annulus, G_{mf} values differ depending upon A_1/A_2 and D_A/D_p for same material. Thus energy requirement which is a function of the velocity can be expressed in terms of Reynold's number (Re). For the materials of the type studied here, the equation is

$$\Delta P_{mf} = 0.78 \left[\frac{W}{A}\right] \left[\frac{D_A}{D_p}\right]^{-0.02} \left[Re_{mf}\right]^{0.04}$$

In the above correlation D_{equ} has been used for calculating R_e. Since the area calculated on the basis of D_{equ} represents the total empty cross-sectional area of annulus through which the fluid flows. The above correlation was obtained on the basis of a regression analysis carried out with the help of IBM 1620 model computer. This correlation should be used only within the range of experimental results reported. Fig. 7.2 shows a plot of experimental versus correlated ΔW and the variation of 85% of the observed values lies within + 7.4 %.

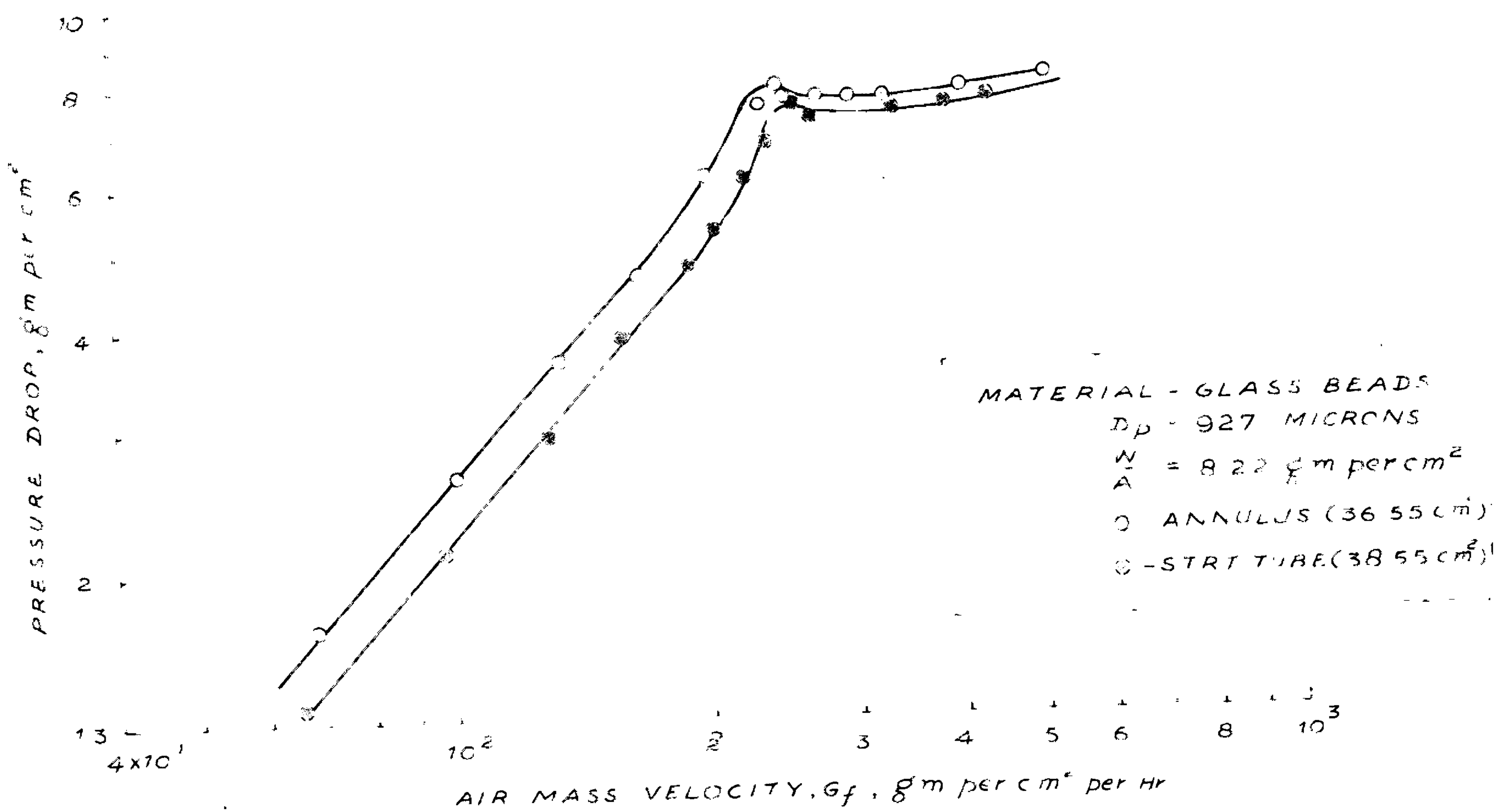

FIG. 6.1 VARIATION OF PRESSURE DROP WITH AIR MASS VELOCITY IN STRAIGHT TUBE AND IN ANNULUS

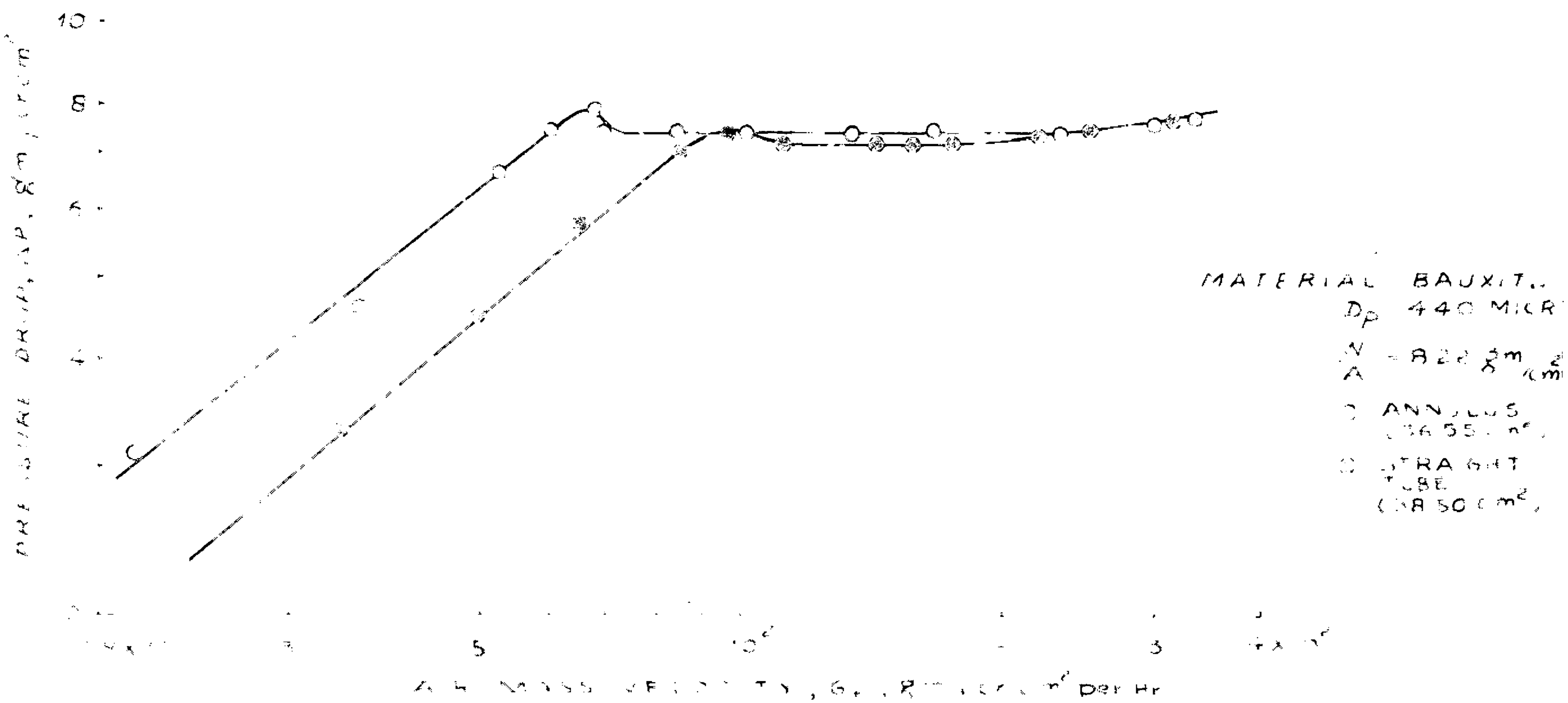

FIG 6.2 VARIATION OF PRESSURE DROP WITH AIR MASS VELOCITY IN STRAIGHT TUBE AND IN ANNULUS

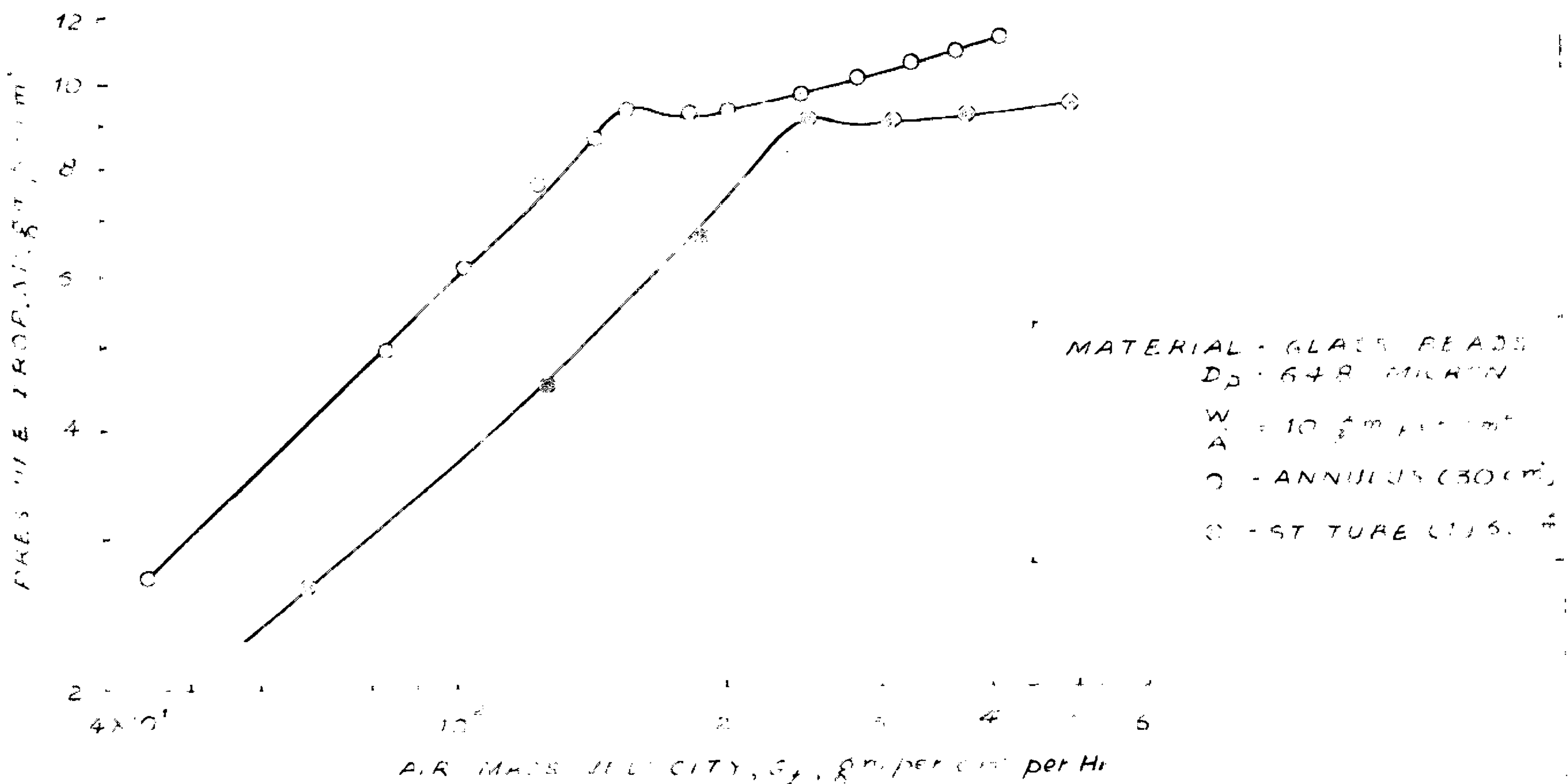

FIG. 6.3 VARIATION OF PRESSURE DROP WITH AIR MASS VELOCITY IN STRAIGHT TUBE AND IN ANNULUS

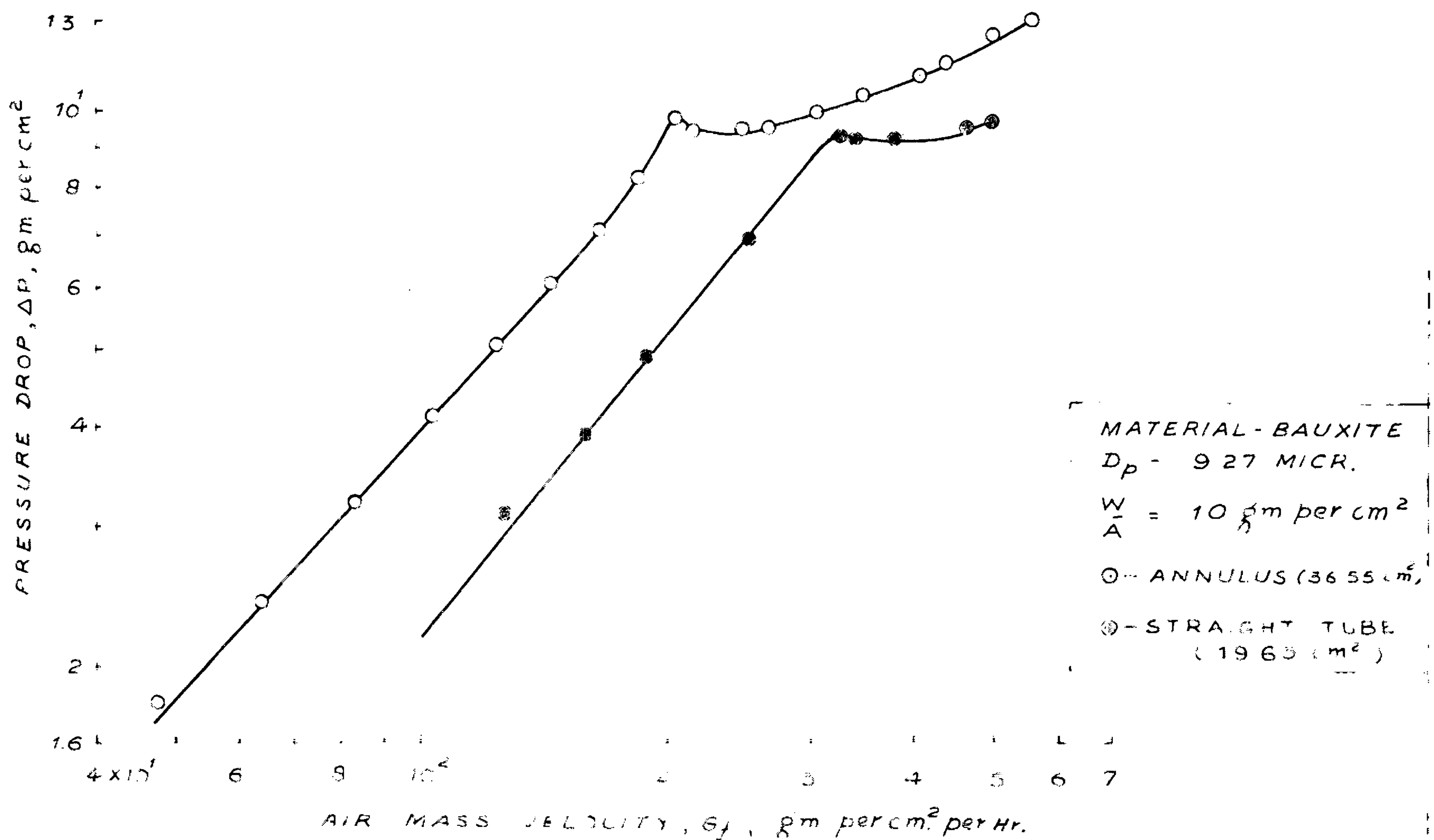

FIG. 6.4 VARIATION OF PRESSURE DROP WITH AIR MASS VELOCITY IN STRAIGHT AND IN ANNULUS

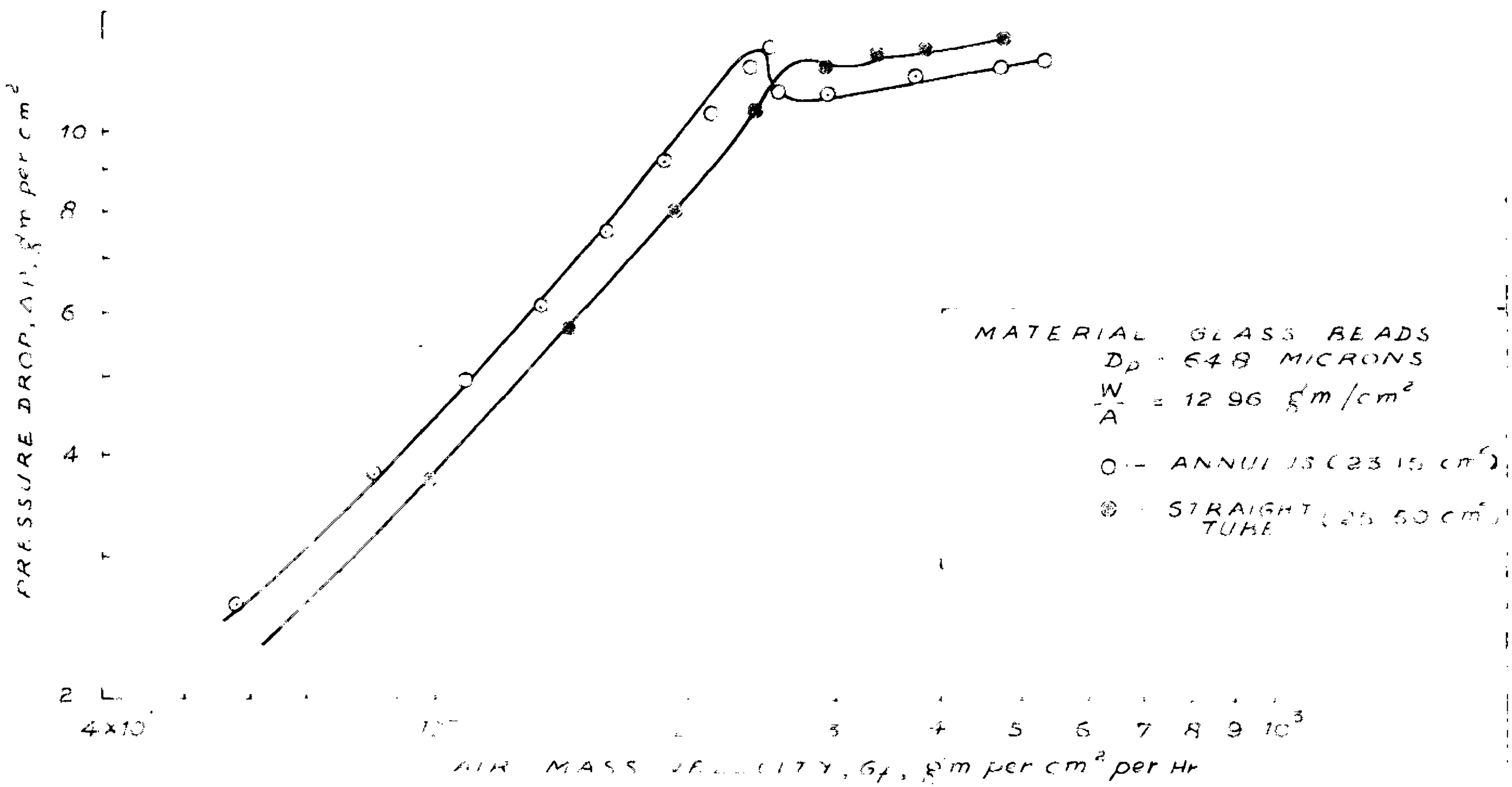

FIG. 6.5 VARIATION OF PRESSURE DROP WITH AIR MASS VELOCITY IN STRAIGHT TUBE AND IN ANNULUS

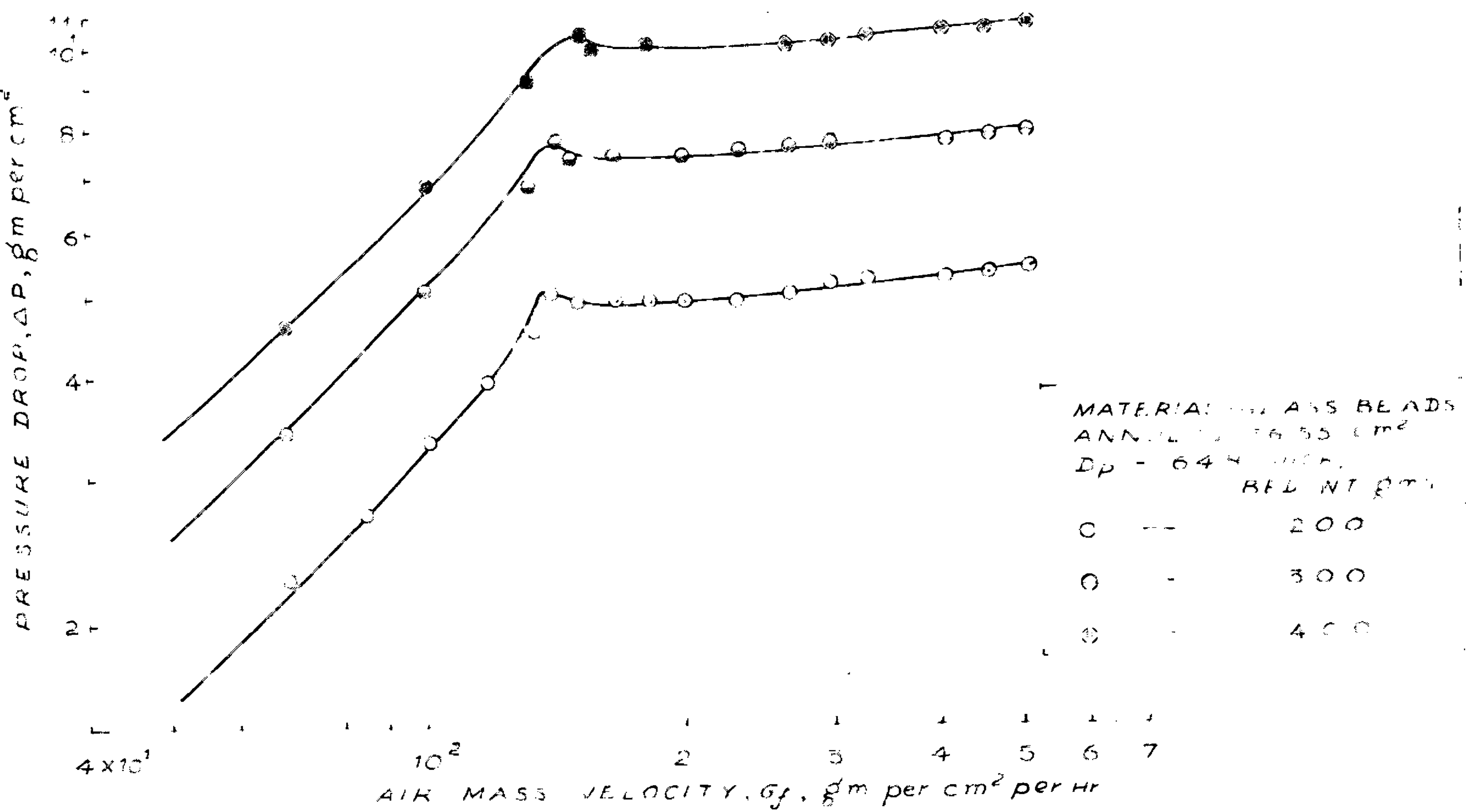

FIG.6.6 VARIATION OF PRESSURE DROP WITH AIR MASS VELOCITY IN ANNULUS

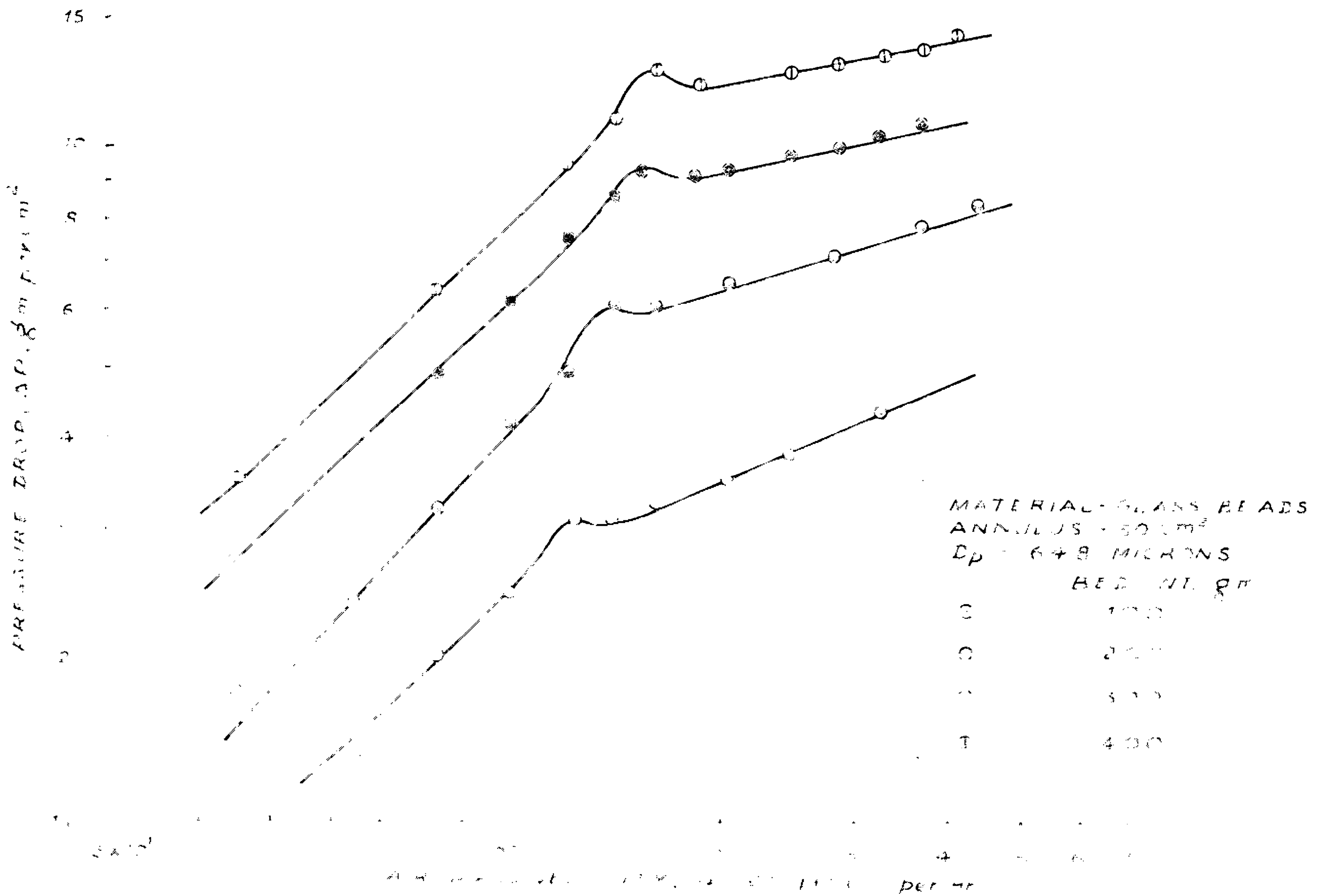

FIG. 67 VARIATION OF PRESSURE DROP WITH AIR MASS VELOCITY IN ANNULUS

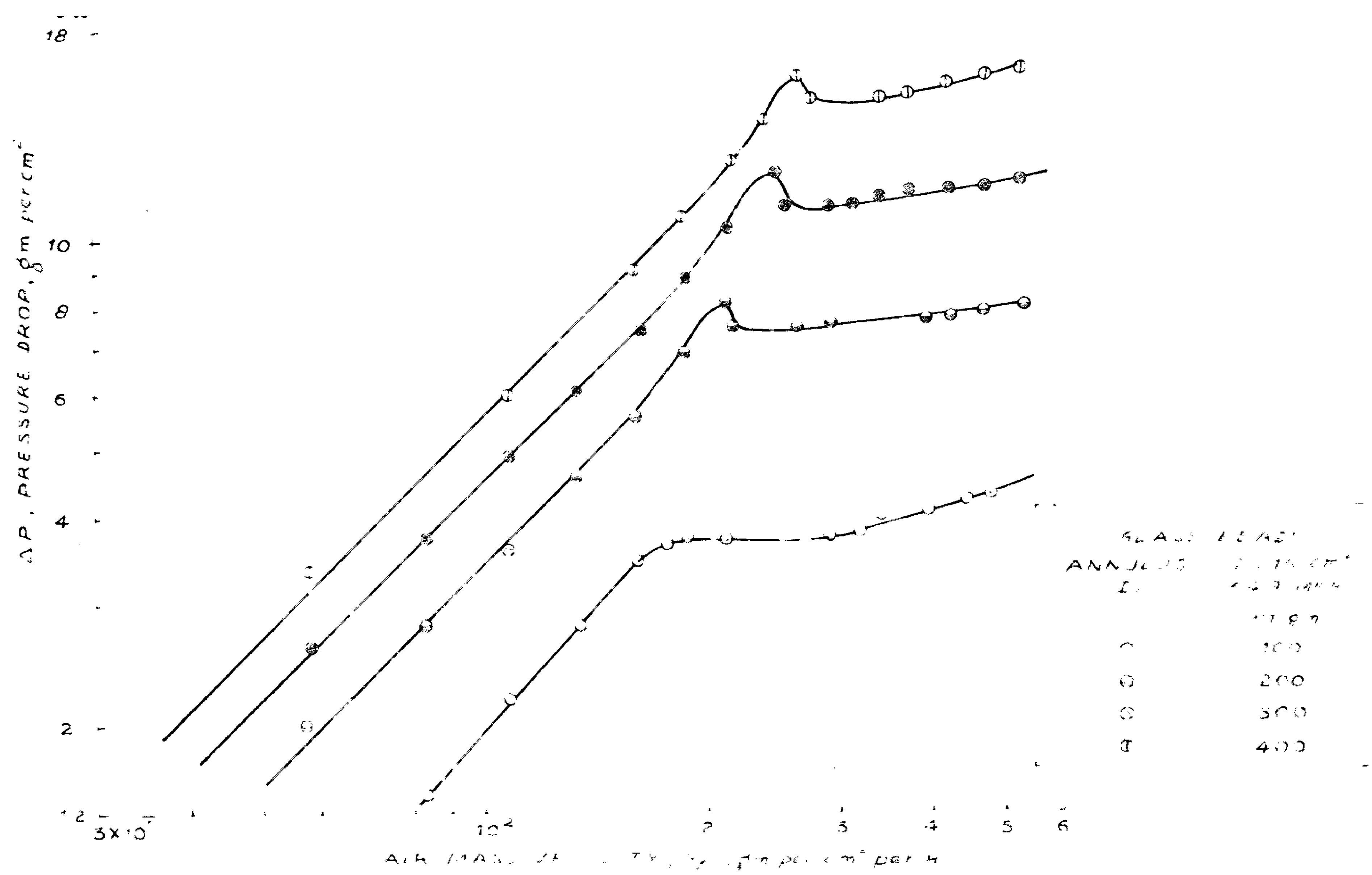

FIG 6.8 VARIATION OF PRESSURE DROP WITH AIR MASS VELOCITY FOR DIFFERENT BED WEIGHTS IN ANNULUS

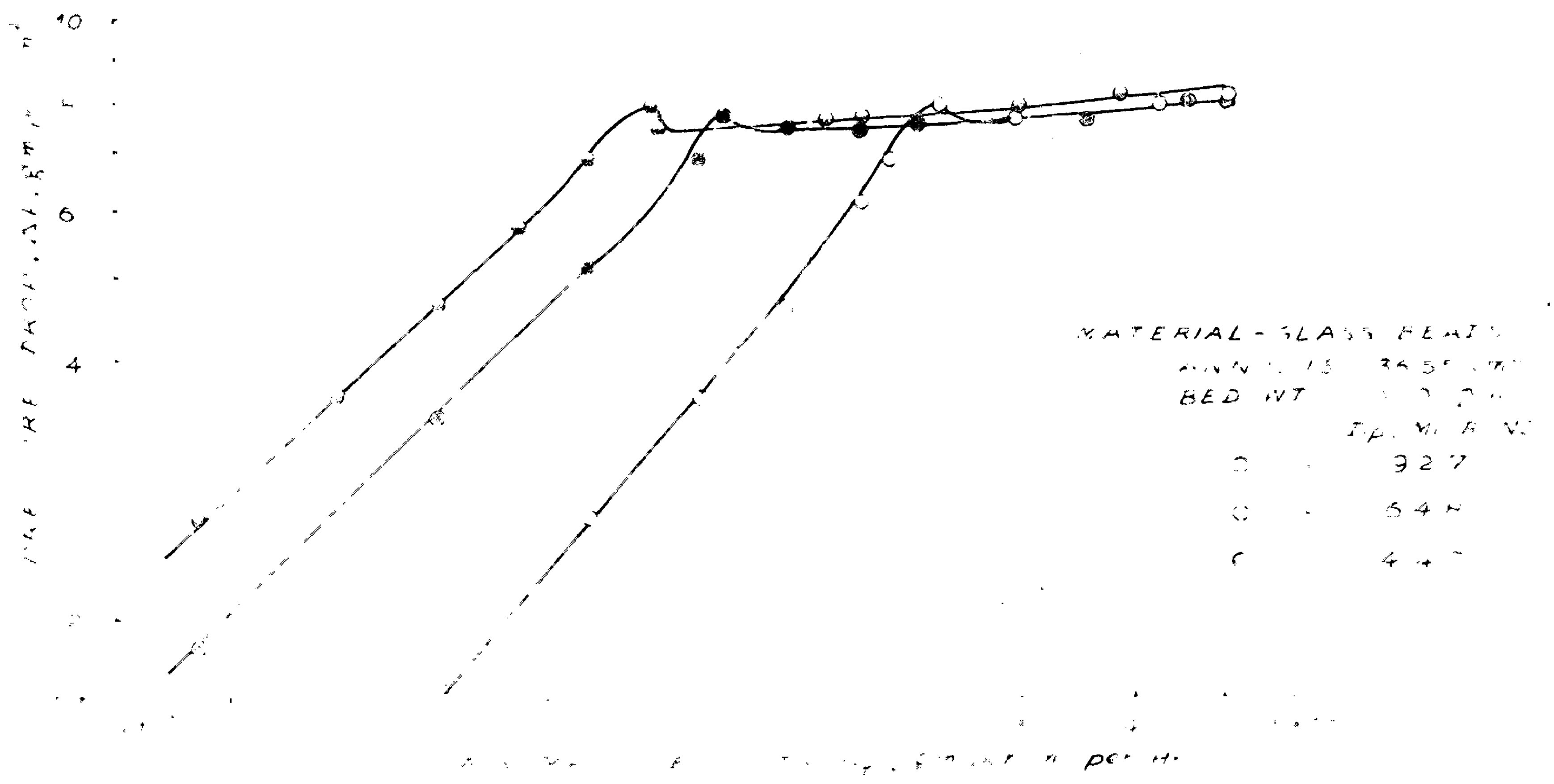

FIG 6.9 VARIATION OF PRESSURE DROP WITH AIR MASS VELOCITY FOR DIFFERENT PARTICLE SIZES IN ANNULUS

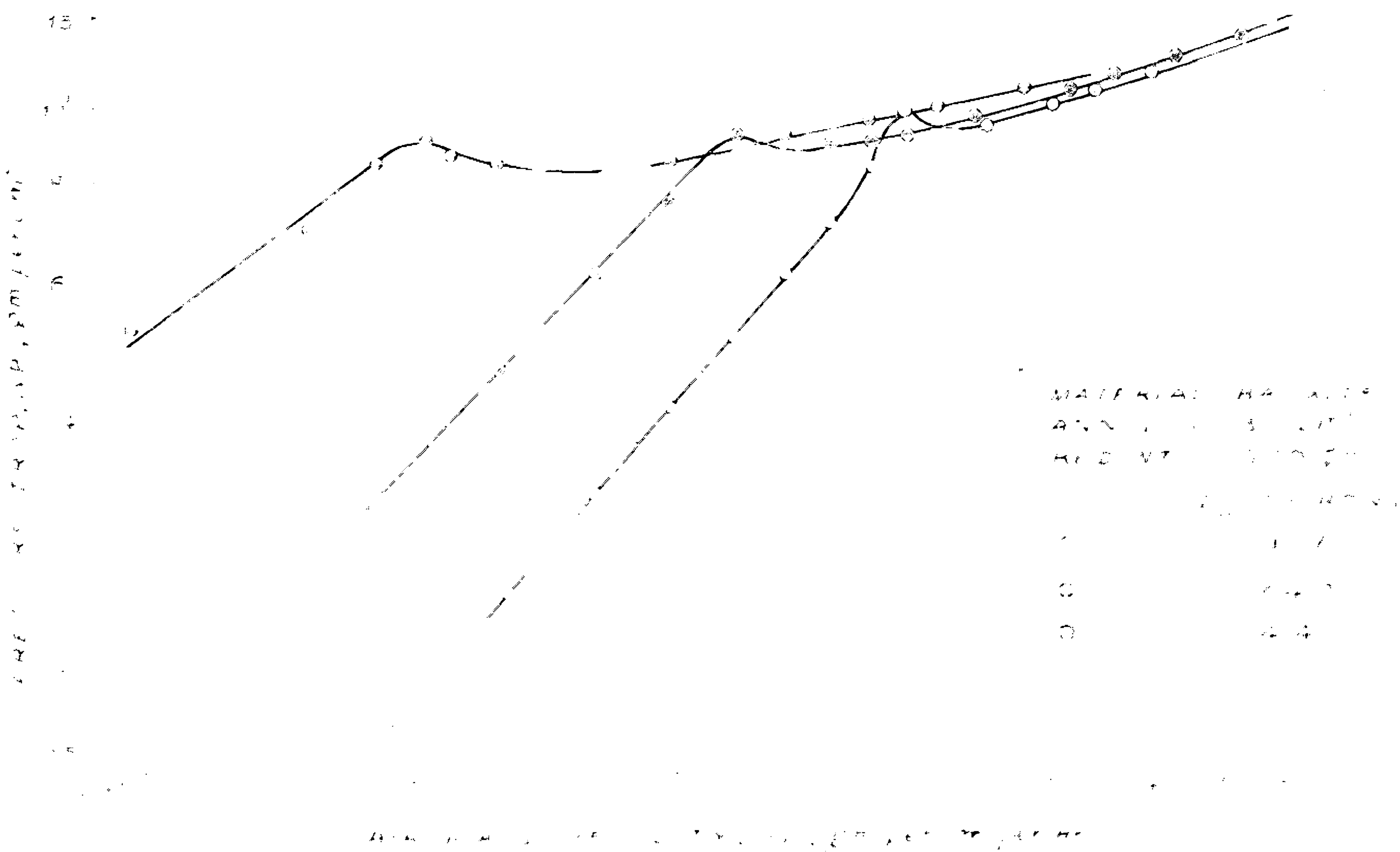

FIG. 6.[illegible] VARIATION OF PRESSURE [illegible] [illegible] MASS VELOCITY
[illegible]

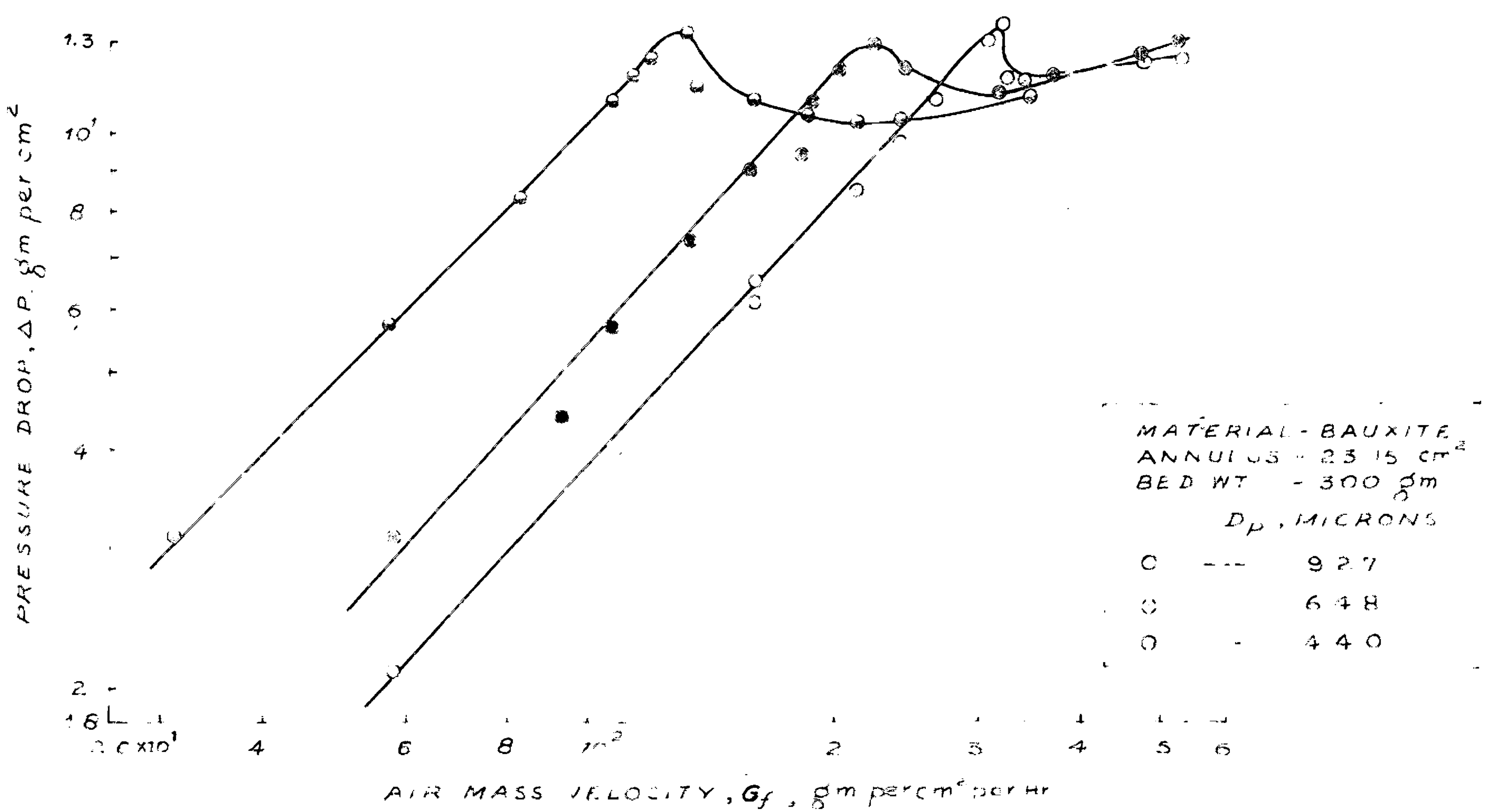

FIG. 6.11 VARIATION OF PRESSURE DROP WITH AIR MASS VELOCITY IN ANNULUS

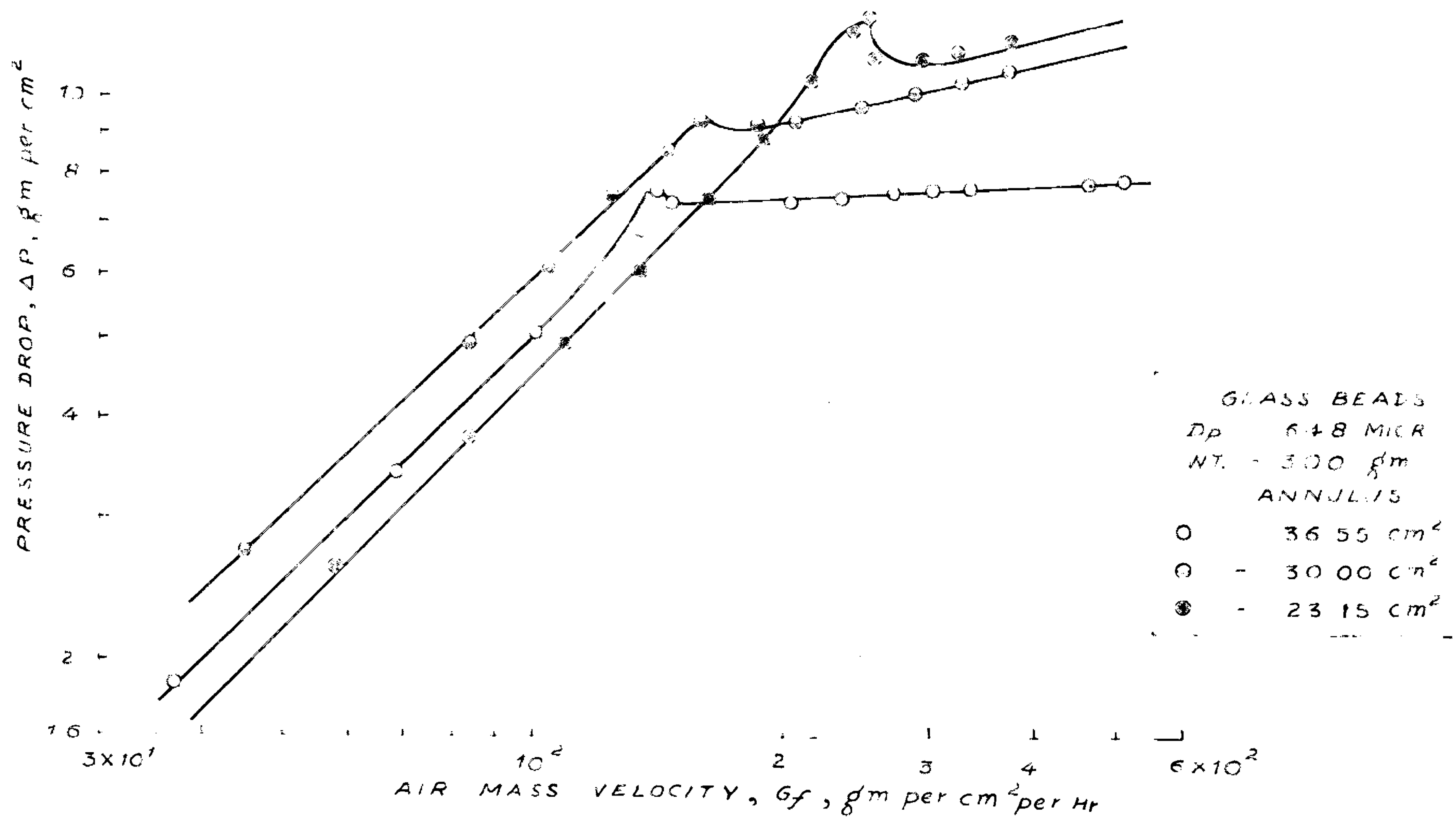

FIG 6.12 VARIATION OF PRESSURE DROP WITH AIR MASS VELOCITY IN DIFFERENT ANNULI

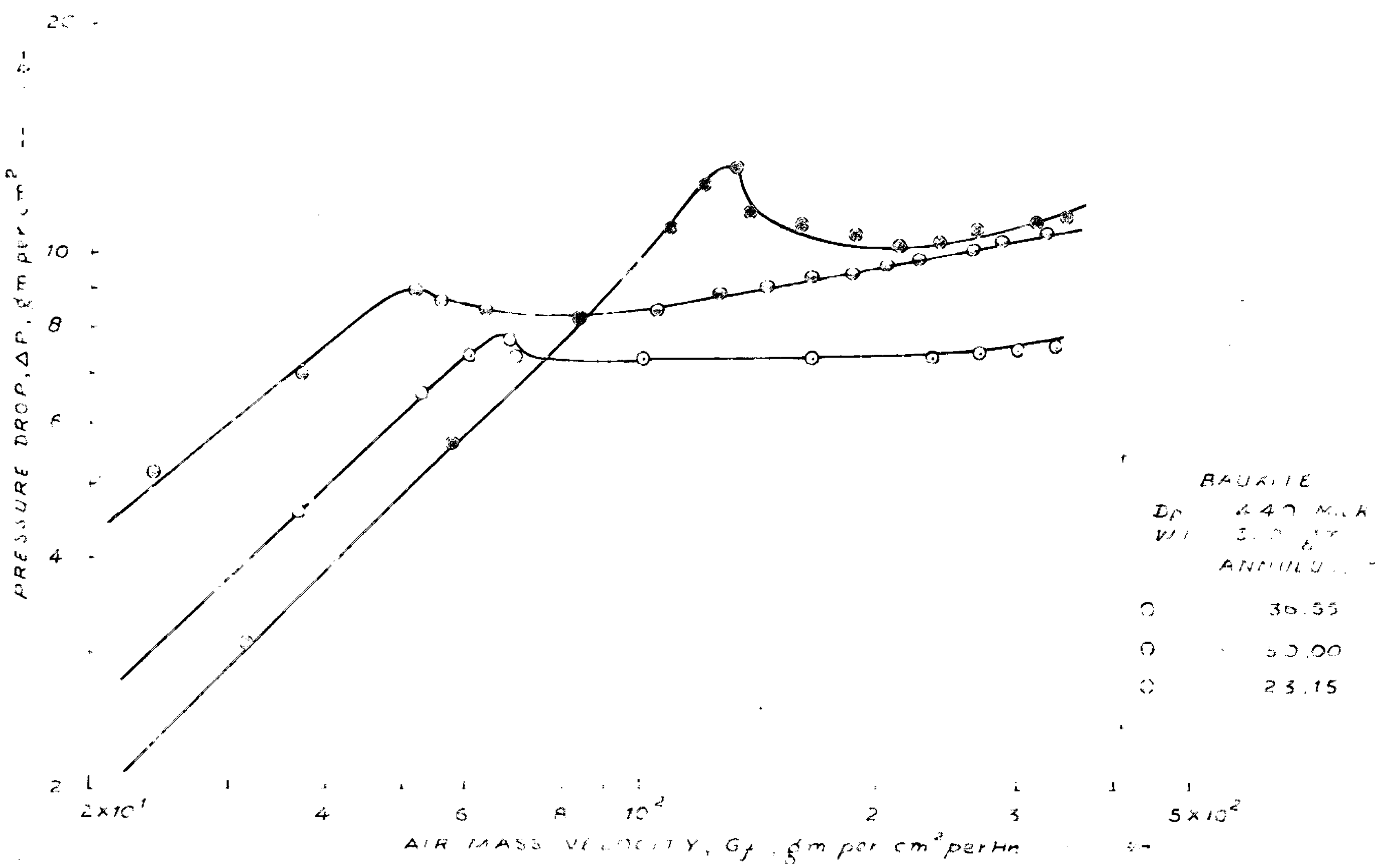

FIG 6.13 VARIATION OF PRESSURE DROP WITH AIR MASS VELOCITY IN DIFFERENT ANNULI

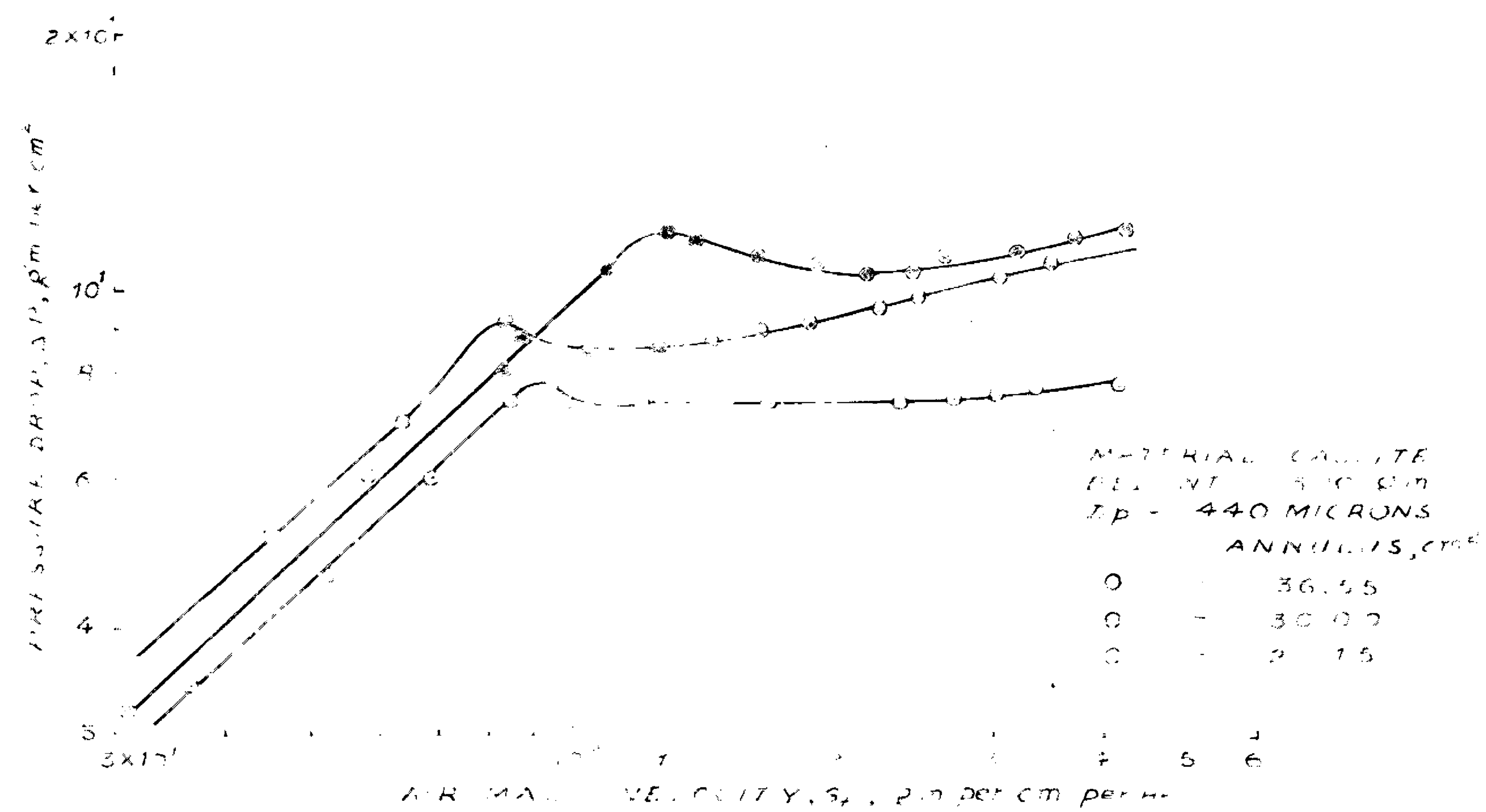

FIG. S.14-VARIATION OF PRESSURE DROP WITH AIR MASS VELOCITY IN DIFFERENT ANNULI

CHAPTER VII

CONCLUSIONS

Fluidizing columns with an inner vertical tube may be used for the purpose of heat removal or addition during chemical reactions. Introduction of such a vertical tube changes the hydrodynamic characteristics. It is observed that the quality of fluidization in an annulus seems to be a strong function of D_A/D_p ratio. Higher is the value of D_A/D_p, greater are the 'channeling' tendencies. On the other hand, lower is the value of D_A/D_p, greater is the 'slugging' phenomenon. There probably is an optimum D_A/D_p ratio where smooth fluidization occurs. Further experimental investigations are required to identify the optimum value of D_A/D_p and hence the zone of smooth fluidization in annulus.

Correlations have been proposed to predict G_{mf} and ΔP_{mf} in annulus which are as follows :

$$(1)\quad \left[\frac{G_{mf\ A}}{G_{mf\ Leva}}\right] = 0.12\left[\frac{D_A}{D_p}\right]^{0.55}\left[\frac{A_1}{A_2}\right]^{-1.90}$$

$$(2)\quad \Delta P_{mf} = 0.78\left[\frac{D_A}{D_p}\right]^{-0.02}\left[Re_{mf}\right]^{0.04}\left[\frac{W}{A}\right]$$

These two correlations are applicable within the range of the following parameters :

(i) $440 < D_p < 927$ Microns

(ii) $2.58 < D_{equ} < 5.42$ cms

(iii) $375 < Re_{mf} < 2165$

(iv) $13.9 < \frac{D_A}{D_p} < 61.5$

(v) $0.602 < \frac{A_1}{A_2} < 0.950$

For obtaining generalized correlations further study is required in the following areas:

1. Larger variation in particle size, D_p
2. Effect of solid and fluid density.
3. Effect of gas distributors
4. Larger number of annuli.

--

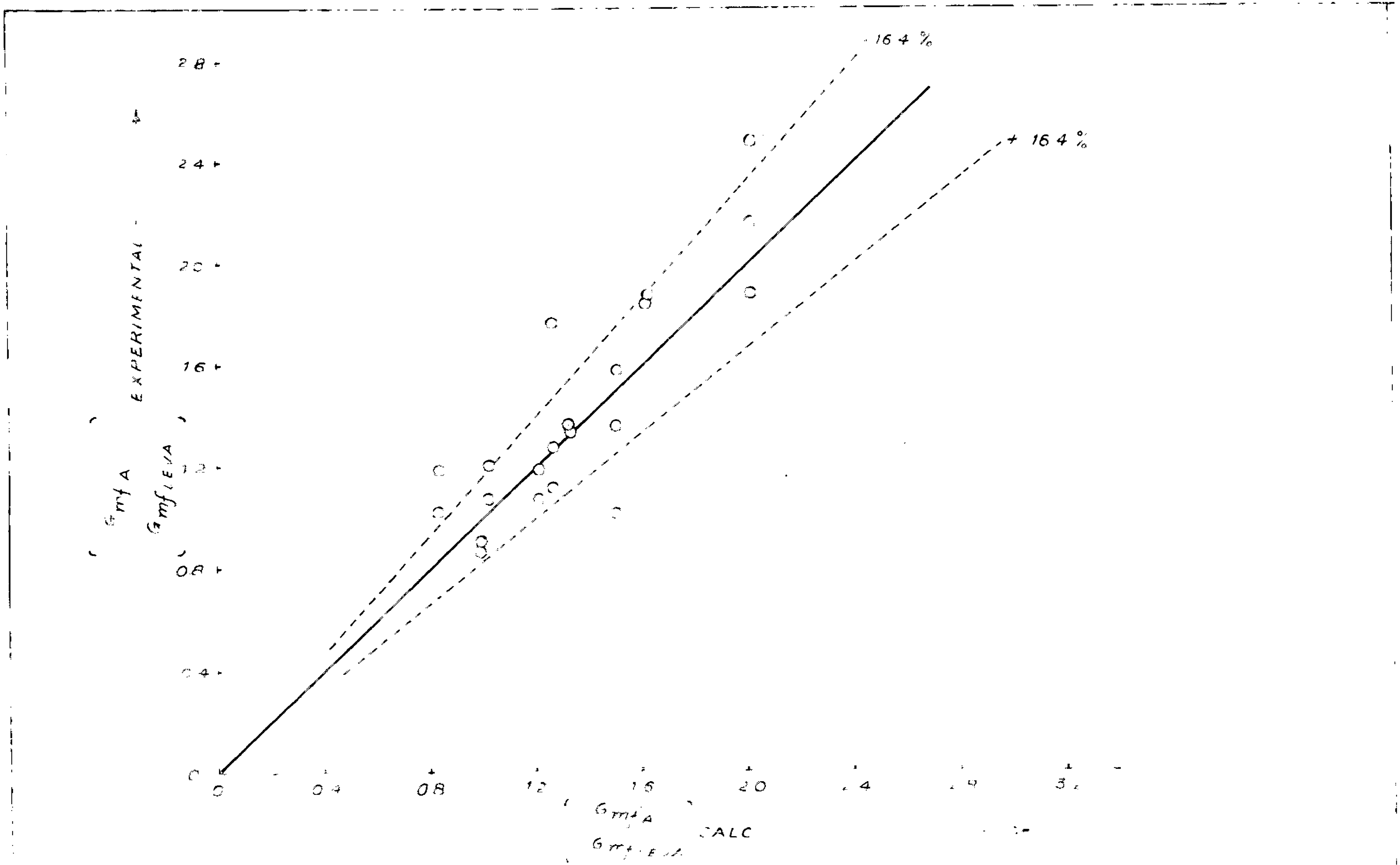

FIG. 7.1 PLOT OF EXPERIMENTAL VS CALCULATED VALUES OF $\frac{G_{mfA}}{G_{mfLEVA}}$

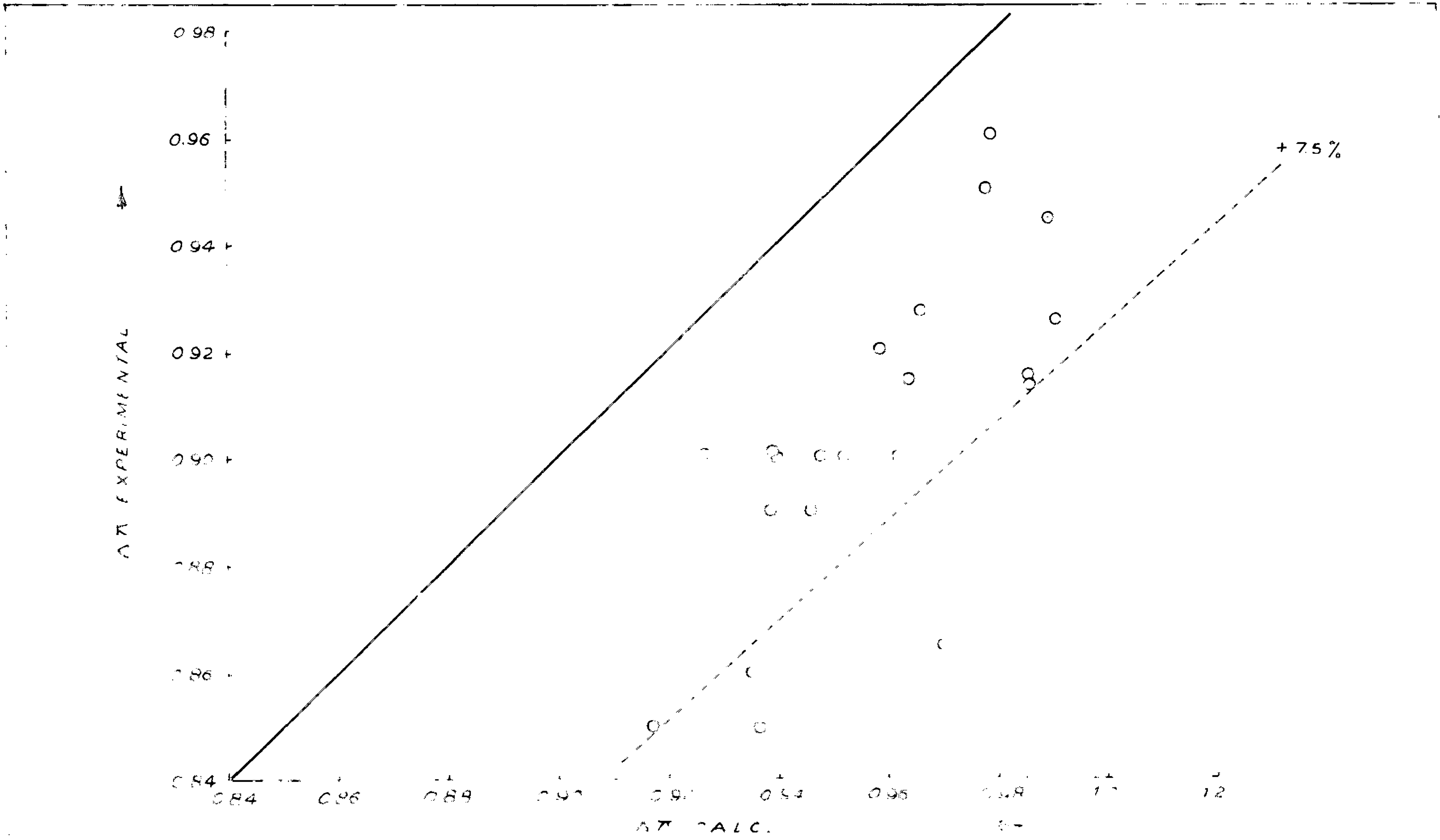

FIG.7.2 PLOT OF EXPERIMENTAL Vs CALCULATED VALUES OF Δπ

APPENDIX

```
C  FLUIDIZATION IN ANNULUS S.S.RAMA KRISHNAN M.E.THESIS U.O.R.
   MINIMUM FLUIDIZATION VELOCITY CORRELATION
   PROGRAMME FOR CURVE FITTING
   DIMENSION X(10,100),Y(10),S(10,11)
   READ 5,L,M
 5 FORMAT(2I10)
   N=L+1
   DO 3J=1,M
   READ 10,(X(I,J),I=1,N)
10 FORMAT(6F12.5)
 3 CONTINUE
   DO 20I=1,N
   DO 20J=1,M
20 X(I,J)=LOGF(X(I,J))
   DO 30I=1,N
   SUM=0.0
   DO 40J=1,M
40 SUM=SUM+X(I,J)
30 Y(I)=SUM
   DO 50I=1,N
   AM=M
   Y(I)=Y(I)/AM
50 CONTINUE
   PUNCH 55,(Y(I),I=1,N)
55 FORMAT(6F12.5)
   DO 60I=1,N
   DO 60J=1,M
60 X(I,J)=X(I,J)-Y(I)
   DO 70I=1,L
   DO 70J=1,N
   S(I,J)=0.0
   DO 70K=1,M
   S(I,J)=S(I,J)+X(I,K)*X(J,K)
70 CONTINUE
   PUNCH 80,((S(I,J),J=1,N),I=1,L)
80 FORMAT(8F9.3)
   STOP
   END
```

2	21	
29.2	0.950	0.926
29.2	0.950	0.970
41.8	0.950	1.200
41.8	0.950	1.070
61.5	0.950	1.270
61.5	0.950	1.160
61.5	0.950	1.760
20.1	0.779	0.895
20.1	0.779	0.864
28.8	0.779	1.070
28.8	0.779	1.180
42.4	0.779	1.358
42.4	0.779	1.005
42.4	0.779	1.570
13.9	0.602	1.330
13.9	0.602	1.360
19.9	0.602	1.040
19.9	0.602	1.875
29.6	0.602	1.080

```
29.4            0.602          2.160
29.4            0.602          2.480


 0.42490      -.26951        .28256
3.960     1.181     -.068     1.181      .732     -.741


C  C  PROGRAMME-TWO DEVIATION FOR MINM.FLU.VELOCITY.CORRELATION.
C     M.E.THESIS.S.S.RAMA KRISHNAN. DEPT.OF CH.E. U.O.R.
      DIMENSIONY(50),YN(50),X1(50),X2(50),YP(50)
      READ5,N
    5 FORMAT(I5)
      READ10,(X1(I),X2(I),Y(I),I=1,N)
C     X1=DA/DP    X2=A1/A2    Y=GMFOBS/GMFLEVA
   10 FORMAT(3F12.5)
      DO20I=1,N
      P=(X1(I))**0.55
      Q=1.0/(X2(I)**1.9)
      YN(I)=0.12*P*Q
      YP(I)=((YN(I)-Y(I))/YN(I))*100.0
   20 CONTINUE
      PUNCH 30,(Y(I),YN(I),YP(I),I=1,N)
   30 FORMAT(3E15.5)
      STOP
      END
   21
    29.2            0.950          0.926
    29.2            0.950          0.970
    41.0            0.950          1.200
    41.0            0.950          1.070
    61.5            0.950          1.270
    61.5            0.950          1.100
    61.5            0.950          1.760
    20.1            0.779          0.895
    20.1            0.779          0.864
    28.0            0.779          1.070
    28.0            0.779          1.180
    42.4            0.779          1.350
    42.4            0.779          1.005
    42.4            0.779          1.370
    19.9            0.602          1.330
    19.9            0.602          1.360
    19.9            0.602          1.840
    19.9            0.602          1.875
    29.4            0.602          1.880
    29.4            0.602          2.160
    29.4            0.602          2.480


C  C  PROGRAMME-TWO DEVIATION FOR MINM.FLU.VELOCITY.CORRELATION.
     0.92600          0.86619          -0.96320E+01
     0.97000          0.86619          -0.15577E+02
     0.12000E+01      0.10307E+01      -0.16420E+02
     0.10700E+01      0.10307E+01      -0.38080E+01
     0.12700E+01      0.12746E+01       0.36401
     0.11000E+01      0.12746E+01       0.13701E+02
     0.17600E+01      0.12746E+01      -0.38078E+02
     0.89500          0.10067E+01       0.10915E+02
```

0.11800E+01	0.12244E+01	0.36269E+01
0.13580E+01	0.15146E+)1	0.10342E+02
0.10050E+01	0.15146E+01	0.33648E+02
0.15700E+01	0.15146E+01	-0.36545E+01
0.13300E+01	0.13385E+01	0.63220
0.13600E+01	0.13385E+01	-0.16092E+01
0.18400E+01	0.16305E+01	-0.12850E+02
0.18750E+01	0.16305E+01	-0.14996E+02
0.18800E+01	0.20209E+01	0.69708E+01
0.21600E+01	0.20209E+01	-0.68846E+01
0.24800E+01	0.20209E+01	-0.22719E+02

0 STOP END AT S. 0030 + 01 L. Z

```
      FLUIDIZATION IN ANNULUS S.S.RAMA KRISHNAN M.E.THESIS U.O.R.
      DIMENSIONLESS PRESSURE DROP CORRELATION
      PROGRAMME FOR CURVE FITTING
      DIMENSION X(10,100),Y(10),S(10,11)
      READ 5,L,M
    5 FORMAT(2I10)
      N=L+1
      DO 9J=1,M
      READ 10,(X(I,J),I=1,N)
   10 FORMAT(6F12.5)
    9 CONTINUE
      DO 20I=1,N
      DO 20J=1,M
   20 X(I,J)=LOGF(X(I,J))
      DO 30I=1,N
      SUM=0.0
      DO 40J=1,M
   40 SUM=SUM+X(I,J)
   30 Y(I)=SUM
      DO 50I=1,N
      AM=M
      Y(I)=Y(I)/AM
   50 CONTINUE
      PUNCH 55,(Y(I),I=1,N)
   55 FORMAT(6F12.5)
      DO 60I=1,N
      DO 60J=1,M
   60 X(I,J)=X(I,J)-Y(I)
      DO 70I=1,L
      DO 70J=1,N
      S(I,J)=0.0
      DO 70K=1,M
      S(I,J)=S(I,J)+X(I,K)*X(J,K)
   70 CONTINUE
      PUNCH 80,((S(I,J),J=1,N),I=1,L)
   80 FORMAT(8F9.3)
      STOP
      END
         2          21
  29.2       1910.            0.914
  29.2       2165.            0.925
  41.8       1295.            0.914
  41.8       1243.            0.900
  61.5        596.            0.900
  61.5       1023.            0.900
  61.5        829.            0.900
  20.1       1270.            0.950
  20.1       1318.            0.960
  28.8        791.            0.900
  28.8        945.            0.920
  42.4        375.            0.850
  42.4        630.            0.850
  42.4        609.            0.860
  13.9       1309.            0.913
  13.9       1432.            0.943
  19.9        942.            0.927
  19.9       1035.            0.865
  29.4        557.            0.890
  29.4        685.            0.890
  29.4        557.            0.905
```

```
 3.42490      6.83884      -.10187
3.960   -1.642   -.143   -1.642    3.980     .199


C  PROGRAMME TWO.DEVIATION FOR PRESSURE DROP CORRELATION
   DIMENSIONY(50),YN(50),X1(50),X2(50),YP(50)
   READ5,N
 5 FORMAT(I5)
   READ10,(X1(I),X2(I),Y(I),I=1,N)
   X1=DA/DP    X2=REMF     Y=DIM.LESS PRESSURE DROP
10 FORMAT(3F12.5)
   DO20I=1,N
   P=1.0/(X1(I)**0.02)
   Q=(X2(I))**0.04
   YN(I)=0.78*P*Q
   YP(I)=((YN(I)-Y(I))/Y(I))*100.0
20 CONTINUE
   PUNCH 30,(Y(I),YN(I),YP(I),I=1,N)
30 FORMAT(3E15.5)
   STOP
   END
21
 29.2      1910.         0.914
 29.2      2165.         0.925
 41.0      1295.         0.914
 41.8      1243.         0.900
 61.5       596.         0.900
 61.5      1023.         0.900
 61.5       829.         0.900
 20.1      1270.         0.950
 20.1      1318.         0.960
 28.0       791.         0.900
 28.8       945.         0.920
 42.4       375.         0.850
 42.4       630.         0.850
 42.4       609.         0.860
 13.9      1309.         0.910
 13.9      1432.         0.943
 19.9       942.         0.927
 19.9      1035.         0.865
 29.4       557.         0.890
 29.4       685.         0.890
 29.4       557.         0.905


C C PROGRAMME TWO.DEVIATION FOR PRESSURE DROP CORRELATION
  0.91400       0.98634       0.73345E+01
  0.92500       0.99130       0.66882E+01
  0.91400       0.96419       0.52052E+01
  0.90000       0.96261       0.65041E+01
  0.90000       0.92753       0.29679E+01
  0.90000       0.94779       0.50423E+01
  0.90000       0.93905       0.42602E+01
  0.95000       0.97765       0.28281E+01
```

0.96000	0.97910	0.19508E+01
0.90000	0.95243	0.35050E+01
0.92000	0.95923	0.40900E+01
0.85000	0.91729	0.73361E+01
0.85000	0.93653	0.92393E+01
0.86000	0.93526	0.80469E+01
0.91300	0.98608	0.74111E+01
0.94300	0.98963	0.47117E+01
0.92700	0.96623	0.40599E+01
0.86500	0.96987	0.10813E+02
0.89000	0.93878	0.51957E+01
0.89000	0.94658	0.59769E+01
0.90500	0.93878	0.33978E+01

0 STOP END AT S. 0030 + 01 L. Z

REFERENCES

1. Morse, R.D. and Ballou, C.O., Chem.Eng.Progr. 47 , 199 (1951).
2. Shuster, W.W. and Kisliak, P., ibid, 48 , 201 (1952).
3. Wilhelm, R.H. and Kwauk, M., ibid, 44 , 201 (1948).
4. Lewis, W.K., Gilliland, E.R. and Bauer, W.C. Ind. Eng. Chem. 41, 1104 (1949).
5. Hancock, R.T., Coke and Gas 386-8(Nov. 1949).
6. Morse, R.D. Ind. Eng. Chem. 41, 117(1949)
7. Schwarts, C.E. and Smith, J.M., Ind. Eng. Chem. 45, No. 6, 1209 (1953).
8. Wen, C.Y. and Yu, Y.H., Chem. Eng. Progr. Symp. Series, 62 (62), 105 (1966).
9. Ergun, S. Chem. Eng. Progr. 48 , 89 (1952)
10. Leva, M., Grummer, M., and Weintraub, M. Chem. Eng. Progr. 44 , 511 (1948).
11. Leva, M. "Fluidisation". McGraw Hill Book Co., Inc., New York (1959).
12. Miller, C.O. and Logwinuk, A.K., Ind. Eng. Chem., 43 , 1221 (1951).
13. Van Heerden, C., Nobel, A.P.P., and Van Krevelen, D.W. Can Jl. Res. 28 , 282 (1950).
14. Narasimhan, G. A.I.Ch.E. Jl. 11 , 550 (1965)
15. Pinchbeck, P.H., and Popper, F. Chem. Eng. Sci. 6 , 57 (1956).

16. Goddard, K.E , and Richardson, J.F. ibid 24, 363 (1969).

17. Frantz, J. Chem. Eng. Progr. Symp. Series, 62 , No. 62, 21(1966).

18. Baerg, A., Klassen, J. and Gishler, P.E., Can. Jl. Research. F. 28, 287 (1950).

19. Pillai, B.C., and Raja Rao, M. Indian Jl. of Tech., 9 , 77 (1971).

20. Balakrishnan, D., and Raja Rao, M., Chem. Proc. and Eng. 5, 6, 17(1971).

21. Murthy, V.S. and Raja Rao, M. Seminar on Recent developments in Ch.E. held at IIT Bombay (1971).

22. Adler, H.L., and Happel, J. Chem. Eng. Progr. Symp. Series., 58 , No. 38, 98(1962).

23. Davidson, J. F. and Harrison, D. " Fluidisation" Academic Press., London (1971).

24. Kunii, D. and Levenspiel, O. Ind. Eng. Chem. Funda. 7, 446 (1968).

25. Grohse, E., A.I.Ch.E. Jl. No.1, 358(1955).

26. Vaneck, D., Markavart, M., and Drobhar, R. "Fluidized bed drying", Leonard Hill London (1966).

27. Zemskov, I.F., Stepnov, A.S. and Denisov, V.F. Khim. Mashinostr. No.6, 21(1960) [As referred to in (26)]

28. Mateson, J. Chem.Eng. Progr. Symp. Series., 66 , 101, 47-51 (1970).

29. Mateson, J.M., Hovmand , S., and Davidson., Chem. Eng. Sci, 24 , 1743 (1969).

30. Ramamurthy, K., and Subba Raju, K. Ind. Eng. Chem. (Process Design and Development) 12 , No. 2, 184-189 (1973).

31. Glass, D.H., and Harrison, D., Chem.Eng. Sci., 19 , 1001 (1964).

32. Glass D.H., Ph.D, Dissertation Univ. of Cambridge, (As referred to in(23)).

33. Morgan, C., Ph.D. dissertation, Univ. of Cambridge, (1967) (as referred to in(23)).

34. Baillie, R.C., Chung, D.S., and Fan, L.T., Ind. Eng. Chem. Funda 2, 245 (1963).

35. Hall, C.C., and Crumbey, P. Jl. App. Chem. 2 , 847(1952).

36. Lewis, W.K., Gilliland, E.R., and Glass, W., A.I.Ch.E. Jl., 5, 419 (1959).

37. Volk, W., Johnson, C.A., and Stotler, H.H., Chem. Eng. Progr. 58 , 44 (1962).

38. Sutherland, K.S. Trans. Inst. Chem. Eng. 39 , 188 (1961).

39. Botterill, J.S.M., Brit. Chem.Eng. 11, 122 (1966).

40. Grace, J.R., and Harrison, D. Triportite Chem.Eng. Conference session 32,Montreal (As referred to in (23)).

41. Botton, R.J., Chem. Eng. Prog. Symp. Series., 66, 8(1970).

42. Hovmand, S., and Davidson, J.F., Trans. Inst. Chem. Eng. 46, 190 (1968).

43. Hebden, D., ibid., 39, 224 (1961).

44. Rowe, P.N., and Stapleton, W.M., ibid. 39, 181 (1961).

45. Agarwal, J.C., and Davis, W.L., Chem. Eng., Progr. Symp. Series, 62, 101 (1966).

46. Hardin, J.B., Chem. Eng. 73, 175(1966).

47. Bhat, G.N., Guconic-Murthy and Weingaertner, E.W., Brit. Chem. Eng. 8, No. 12, 813 (1963).

48. Agarwal, O.P. and Storrow, J.A., Chem. and Ind. (Lond) 278(1958).

49. Leva, M. Grummer, M. Weintraub, M. and Storch. Chem. Eng. Progr. 44, 707(1948).

50. Oman, A.O. and Watson, K.M. Natl. Petrol. News 36, R795(1944). (As referred to in (47)).

--